iEnergy
REVIEW
https://doi.org/10.23919/IEN.2022.0008

Recent progress on dielectric polymers and composites for capacitive energy storage

Zhubing Han and Qing Wang ✉

ABSTRACT

Polymer dielectrics-based capacitors are indispensable to the development of increasingly complex, miniaturized and sustainable electronics and electrical systems. However, the current polymer dielectrics are limited by their relatively low discharged energy density, efficiency and poor high-temperature performance. Here, we review the recent advances in the development of high-performance polymer and composite dielectrics for capacitive energy storage applications at both ambient and elevated temperature (≥ 150 °C). We highlight the underlying rationale behind the material development by constructing the relationship between the physical properties of materials and their energy-storage capability. Challenges and future opportunities are discussed at the end of the review.

KEYWORDS

Energy storage, capacitors, dielectric polymers, composite dielectrics.

A capacitor is a type of energy storage device that can release electrical energy instantly to achieve a high power density[1]. The structure of a simple thin-film dielectric capacitor comprises a thin layer of a dielectric material placed between two conducting electrodes. Under an electric field, an equal amount of opposite charges accumulate on each side of the dielectric material, and a high-power pulse is generated upon the release of the stored electrical energy. Compared with other energy storage devices such as batteries and supercapacitors, dielectric capacitors are known for their high power density (> 106 W/kg) but low energy density (< 100 W/kg specific power)[2]. The high power density is a result of extremely fast discharging speed (< 0.01 s) since there is no electrochemical process involved in the charge-discharge cycles. Dielectric capacitors are the essential components in many electrical devices and systems, from small personal appliances such as cellphones and laptops to large systems like hybrid/electric vehicles and powers grids[3,4].

The property of the dielectric materials dominates the key characteristics of the capacitors, such as energy density, power density and charge-discharge efficiency. In the last few decades, the emergence of increasingly complex, flexible and miniature electronics and electrical systems requires high-performance and small-size capacitors that are also reliable and cost-effective. To this end, polymer and composite dielectrics have been the subject of intensive research interests due to their unparalleled advantages over the inorganic counterparts such as high energy density, high breakdown strength and graceful failure behavior[5–13]. Their excellent flexibility and processibility enable facile manufacturing of high quality and large-area films by extrusion, solution casting, electrospinning and high throughput roll-to-roll manufacturing techniques. In addition, they can also be readily assembled into hierarchical (such as sandwiched or multilayered) structures[14]. These features make them attractive for the development of high-performance, low-cost and reliable dielectric capacitors. The dielectric properties and energy storage performance of some representative polymers and ceramics are compared in Table 1.

The capacitive performance of a dielectric material is quantitively evaluated by several parameters, including energy density, power density, charge-discharge efficiency, etc. These parameters are related to the fundamental physical properties of the dielectric materials. High energy density is one of the most sought-after properties in developing high-performance polymer dielectrics. High energy density can significantly reduce the space and weight brought by the capacitors and accessory components. The storage energy density, U_s, is often expressed as the electrical energy stored per unit volume (J/cm^3), which can be calculated from[7]:

$$U_s = \int E\mathrm{d}D \tag{1}$$

where E is the electric field between the electrodes and D is the induced electric displacement of the dielectric material. For a linear dielectric material, whose dielectric constant K (also called relative permittivity ε_r) does not vary with the electric field, the equation can be simplified as:

$$U_s = \frac{1}{2}\varepsilon_0 K E^2 \tag{2}$$

where ε_0 is the vacuum permittivity (= 8.854 × 10^{-12} F/m) and E is the applied electric field. The highest electric field that can be applied to a dielectric material is largely determined by its breakdown strength E_b. Biaxially oriented polypropylene (BOPP), is the current commercial benchmark for polymer film capacitors[16]. PP is a semicrystalline polymer, and its chemical structure can be represented as -[$CH_2CH(CH_3)$]$_n$-. As a linear dielectric material, BOPP is known for the low dielectric loss (~0.02%) and high breakdown strength (> 700 MV/m). However, its low dielectric constant (K = 2.2) leads to a rather small energy density (< 5 J/cm^3), which cannot meet the growing demand for high-performance dielectric capacitors.

Department of Materials Science and Engineering, The Pennsylvania State University, University Park, PA 16802, USA
Address correspondence to Qing Wang, wang@matse.psu.edu

Table 1 Dielectric properties and energy storage performance of select polymers and ceramics materials at room temperature

Materials	K @ 1 kHz	tanδ @ 1 kHz	U_e (J/cm^3)	η (%)
Polymers				
PP[15,16]	2.2	0.0002	2–3 @ ~500 MV/m	
PVDF[17,18]	~10	~0.02	γ phase: 14 @ 500 MV/m98% β-phase: 35 @ 880 MV/m	74
P(VDF-CTFE) 91/9[19]	13	0.03	25 @ 600 MV/m	
P(VDF-HFP) 95.5/4.5[20]	~13		>25 @ 700 MV/m	
P(VDF-BTFE)[21]	12.8	0.025	20.8 @ 750 MV/m	
P(VDF-TrFE-CFE)[22]	>50	~0.08	~10 @ 350 MV/m	
P(VDF-TrFE-CTFE)[23,24]	>50		~13 @ 500 MV/m	>60
Ceramics				
$0.9CaTiO_3$-$0.1BiScO_3$ [25]	172	0.003	1.55 @ 27 MV/m	90.4
$BaTiO_3$ [26]	2000		5 @ 80 MV/m	
$0.7BaTiO_3$-$0.3BiScO_3$[27]	650 (10 kHz)	0.15 (10 kHz)	6.1 @ 73 MV/m	
$(BiFeO_3)_{0.4}$–$(SrTiO_3)_{0.6}$[28]	~930	~0.04	18.6 @ 97.2 MV/m	>85
$Pb_{0.97}Y_{0.02}[(Zr_{0.6}Sn_{0.4})_{0.925}Ti_{0.075}]O_3$[29]			21.0 @ 130 MV/m	91.9
$Ba_{0.53}Sr_{0.47}TiO_3$-based multilayers[30]	~300 (100 Hz)	<0.07 (100 Hz)	51.2 @ 480 MV/m	~35

It can be seen from the Eq. (2) that, from a material perspective, high dielectric constant and breakdown strength are critically desired to achieve a high energy density. A number of high K ferroelectric polymers and nanocomposites have been developed to show significantly enhanced energy density[8]. However, a material with a high dielectric constant does not necessarily guarantee a high discharged energy due to the inefficient discharging process, which can be attributed to dielectric loss, conduction loss or polarization hysteresis in ferroelectric materials. The dielectric loss tangent (tanδ), also known as dissipation factor (DF) or simply dielectric loss, describes the dissipation of the electrical energy over the charging-discharging process. Although many linear dielectrics show little dielectric loss at room temperature, the conduction loss becomes predominant at elevated temperature and high electric field. In practice, the discharged energy density (U_e) is often calculated from the unipolar displacement-electric field (D-E) loop (Figure 1), and the charge-discharge efficiency η, is defined as the ratio between the discharged energy density and storage energy density, i.e, $\eta = U_e/U_s$. Not only does a low efficiency compromises the discharged energy density, but more importantly, the dielectric and conduction loss can cause the generation of Joule heat during the operation of the device, which may lead to thermal runaway and catastrophic failure of the device.

High breakdown strength is another important factor as the energy density scales quadratically with the electric field. For polymer dielectrics, there are three main breakdown mechanisms[31,32]. Free volume breakdown happens as the electrons are accelerated under the electric field and the high-speed electrons collide with the polymer chains. The thermal breakdown is a result of accumulated heat generated from the dissipated energy from dielectric loss and conduction. The mechanical breakdown occurs when the mechanic deformation, which is a result of the electrostatic attraction, exceeds the compressive mechanical strength of the material. This phenomenon is more concerning in soft dielectrics such as polymers with low Young's modulus. In general, polymer dielectrics with rigid backbones exhibit higher Young's modulus (> 2 GPa) than the linear ferroelectric polymers (hundreds of MPa for PVDF-based terpolymers). Many strategies have been proposed to improve the breakdown strength, such as reducing the free volume, incorporating insulating fillers or layers, adding nanofillers with high thermal conductivity and improving the Young's modulus.

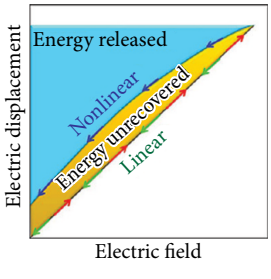

Fig. 1 Schematic representation of the unipolar D-E hysteresis loop of a linear and nonlinear dielectric polymer. The area in blue represents the discharged energy density (reprinted with permission from Ref. [6], © 2012 American Chemical Society).

In addition to the energy density, an important but often underreported parameter for capacitors is the power density, which is essentially the discharged energy density per unit time. In many cases, the main function of capacitors is to provide a high-power pulse instead of working as an energy reservoir like batteries. Therefore, the ability to release high energy density in a short period of time is important for practical applications. In most reports, the discharge time is often selected when the discharged energy in a load resistor achieves 90% or 95% of the final value.

While most conventional approaches focus on the room temperature energy storage properties of polymer dielectrics, there is a growing demand to develop polymer dielectrics that can operate at excessively high temperature as many capacitors are required to work in harsh conditions[11–13]. For example, the near-engine temperature in hybrid electric vehicles can reach 140–150 °C[4], and the working temperature can even reach 200 or 250 °C in underground oil and gas exploration or aircrafts[33]. Most commercially available polymers cannot operate under such high temperature without an effective cooling system, which adds additional weight and volume. To address this problem, polymers with high glass transition temperature (T_g) and their composites are the promising candidates to achieve a decent energy density while main-

taining a high efficiency and low electrical conduction at high temperature and electric field. It is noted that currently there is no clear definition on the exact temperature for high-temperature energy storage, but most literatures in this field will report the energy storage performance at 150 °C or above.

The last few years have witnessed exciting progress on the development of dielectric polymers and composites for capacitive energy storage. This review will start with the state-of-art polymer-based dielectrics for room-temperature applications, including high-*K* ferroelectrics, composites and linear dielectrics. The second part is dedicated to the recent development of polymer and composite dielectrics for high temperature applications. We will summarize the universal and unique strategies to achieve high energy-storage performance at various conditions. Emphasis is on how the interplay of different factors should be considered during the material design process. The challenges and future outlook are included in the last part of this article.

1 Polymers and composites for room temperature energy storage

1.1 Ferroelectric fluoropolymers

Compared with semicrystalline nonpolar polymers and amorphous polar polymers, ferroelectric polymers are characterized by the switchable permanent dipoles and the high dielectric constant[34]. The most notable examples of ferroelectric polymers include PVDF and its copolymers due to their highest dielectric constant among polymers and tunable dielectric properties. PVDF is a semicrystalline polymer whose chemical structure can be represented as -$(CF_2$-$CH_2)_n$-. The exceptional dielectric property of PVDF stems from the arrangement of highly polarized C–F bonds in the crystals. At least five different crystal structures have been reported in PVDF, depending on the chain conformation (trans, T or gauche, G) and how the molecules are packed in the crystalline phase[35]. The polar β phase, where the molecular chains are in an all-trans fashion, exhibits the highest electroactivity. However, direct crystallization of PVDF from the solution or melt often gives rise a majority of non-ferroelectric α phase, in which polymer chains adopt a TGTG' conformation. Electrical poling and mechanical stretching at elevated temperature are necessary to align the dipoles and transform the paraelectric α phase to the ferroelectric β phase these. Introducing bulky trifluoroethylene (TrFE) is another way to induce the formation of polar phase by stabilizing the all-trans conformation[36]. The resulted random copolymer P(VDF-TrFE) with TrFE content > 20 mol% can directly crystallizes into the polar phase and exhibits a detectable Curie transition temperature, and its properties are highly dependent on the composition.

Despite the high dielectric constant (K > 10) of β-PVDF and P(VDF-TrFE) copolymer, their energy density is relatively low due to large ferroelectric hysteresis. Li et al. systematically investigated the energy storage performance of different forms of PVDF[17]. It is found that γ-PVDF shows the highest energy density of 14 J/cm^3 under 500 MV/m electric field, whereas α phase can only exist stably under 300 MV/m, beyond which a phase transition to γ-phase occurs. Ferroelectric β-PVDF shows an unsurprisingly low discharged energy density of 1.5 J/cm^3 at 150 MV/m due to the large remanent polarization and early saturation. In 2019, Meng et al. reported a record high energy density of 35 J/cm^3 and an efficiency of 74% at 880 MV/m on PVDF with extremely high β content (~98% of crystalline phase)[18]. The unusually high β phase is obtained from a repetitive press-and-folding (P&F) process, and the applied pressure results in a close-packing of atoms and favors the formation of β phase which has a smaller unit cell volume. Interestingly, relaxor-like behavior such as a slim *P-E* loop is observed on the P&F PVDF films with high molecular weight. This contradicts to the conventional conception that high β phase content should give rise to a large ferroelectric hysteresis. This peculiar phenomenon is attributed to the unstable small-sized polar structures that are able to reverse upon the decrease of the electric field.

It is intuitive to improve the discharge efficiency of PVDF and P(VDF-TrFE) by eliminating the ferroelectric hysteresis effect. By introducing structural defects, a number of high-*K* relaxor ferroelectric polymers have been developed, such as electron-irradiated P(VDF-TrFE), P(VDF-TrFE-CFE) (CFE: chlorofluoroethylene) and P(VDF-TrFE-CTFE) (CTFE: chlorotrifluoroethylene)[22–24, 37]. The e-beam irradiation or incorporation of a bulky chlorinated comonomer disrupts the long-range ferroelectric domains and facilitates the formation polar nanoregions, and thus a diminished polarization hysteresis is observed. For example, an energy density of ~10 J/cm^3 is measured at 350 MV/m on P(VDF-TrFE-CFE) terpolymer (K > 50 @ 1 kHz)[22]. Another relaxor ferroelectric terpolymer, P(VDF-TrFE-CTFE) with a composition of 65.6/26.7/7.7 mol%, exhibits an energy density of 13 J/cm^3 at the breakdown field of > 500 MV/m[23, 24].

One issue concerning the high-*K* relaxor ferroelectric polymers is that their polarization saturates at relatively low electric field. An important argument by Chu et al. states that avoiding early polarization saturation and a moderate dielectric constant are more important than a very high dielectric constant at low field in order to maximize energy density[38]. For example, P(VDF-CTFE) 91/9 mol% copolymer exhibits a discharged energy density of 17 J/cm^3 at 575 MV/m, outperforming the ferroelectric relaxor P(VDF-TrFE-CFE) (U_e~9 J/cm^3 at 400 MV/m), although the latter one has a much larger low-field dielectric constant and a slimmer *D-E* loop. The CTFE in the copolymer eases the energy barrier of conformational changes between polar and nonpolar phases. An even higher energy density of 25 J/cm^3 is measured at 600 MV/m on extruded P(VDF-CTFE) films[19]. Moreover, P(VDF-TrFE) networks made from photo or chemical crosslinking were also reported to retain a high energy density while lowering the dielectric loss[39, 40]. A discharged energy density of 17 J/cm^3 and an efficiency of 83% are obtained on the crosslinked P(VDF-CTFE) at 400 MV/m, compared with the < 65 % efficiency of the pristine copolymer films. In addition to CTFE, larger size defects such as hexafluoropropylene (HFP) and bromotrifluoroethylene (BTFE) have also been introduced into PVDF to develop high energy density polymer dielectrics[20, 21, 41]. P(VDF-HFP) 95.5/4.5 mol copolymer exhibits a room temperature energy density larger than 25 J/cm^3 under 700 MV/m, while an energy density of 20.8 J/cm^3 is measured at P(VDF-BTFE) with 0.5 mol% BTFE at 716 MV/m.

1.2 Ferroelectric nanocomposites

Over the past two decades, a wide range of nanosized fillers have been blended with ferroelectric polymers in an attempt to enhance the energy storage performance[9, 11, 42, 43]. These nanofillers have varying chemical compositions (inorganic ceramics, oxides organic molecules, 2D materials, polymers) and dimensions (0D nanoparticles, 1D nanorods or nanowires, 2D nanosheets). In general, the functions of these nanofillers include improving dielectric constant, reducing conduction loss, improving Young's modulus and facilitating heat conduction. The improved Young's

modulus is beneficial to the breakdown strength of the material. Meanwhile, the addition of nanofillers, especially at high loading ratios, may lead to adverse effects such as reduced tensile strength, increased brittleness and poor processibility. Therefore, the concentration and dispersion of the nanofillers should be carefully investigated to consider the tradeoff between the dielectric properties and film quality of the composite dielectrics. Recent progress often involves a more complex material design, such as hierarchically structured nanofillers, multi-component nanocomposites and layered nanocomposites. The dielectric properties and energy storage performance of ferroelectric polymer-based nanocomposite developed in the recent years are listed in Table 2.

1.2.1 *Nanocomposites with high-K ceramic nanofillers*

The energy density of a dielectric nanocomposite can be regarded as the volumetric summation of the energy density of each component plus the effect of the interfacial region, i.e., $U = f_1U^{(1)}+f_2U^{(2)}+gU^{(3)}$, where U is the overall energy density, f_1 and f_2 are the volume fraction of the filler and the polymer, respectively, and g is the interfacial area between the two components[9]. As early as in 2000, Bai et al. reported that nanocomposites composed of P(VDF-TrFE) 50/50 mol% and $Pb(Mg_{1/3}Nb_{2/3})O_3$–$PbTiO_3$ (PMN-PT) powders show a high dielectric constant of 250 and a maximum energy density of 15 J/cm³ at the breakdown field of 120 MV/m[44].

$BaTiO_3$ (BT) is one of the most popular ceramic fillers to form composites with ferroelectric polymers owing to its high K and wide accessibility[45–55]. Un-treated BT nanoparticles are prone to aggregation, which leads to poor film quality and reduced breakdown strength. Surface modification with organic ligands or polymers is often employed to ensure the homogenous dispersion of the nanomaterials into the polymer matrix and to mitigate the large dielectric constant difference on the polymer-nanofiller interface. For example, Luo et al. reported a nanocomposite composed of P(VDF-HFP) and BT nanoparticles coated with hydantoin epoxy resin[50]. The surface functionalization ensures the homogeneous dispersion of BT nanoparticles even at very high loading content. The composite with 20 vol% of BT nanoparticles exhibits the highest energy density of 8.13 J/cm³. One problem of the traditional surface-functionalization approach is that high loading ratio of BT nanoparticles is often necessary to obtain a high K at a price of much degraded breakdown strength (< 100 MV/m)[45]. To address this issue, strong interactions (hydrogen bonding and chemical bonding) are often introduced between the nanoparticles and the polymer matrix. Xie et al. reported a solution-processed network composite made from P(VDF-CTFE) with internal double bonds (P(VDF-CTFE-DB)) and BT nanoparticles modified with polydopamine (PDA), and the crosslinking reaction is initiated by benzoperoxide (Figure 2(a))[52]. Owing to the crosslinked polymer network and the hydrogen bonding between the nanoparticles and the polymer matrix, this composite exhibits an increased Young's modulus (Figure 2(b)). A high dielectric constant of 30 and improved breakdown strength (300 MV/m) are also observed. As shown in Figures 2(c) and 2(d), the *c*-PVDF/PDA@BT nanocomposite with 2.0 wt% filler content exhibits an energy density of 2.9 J/cm³. Most recently, Ma et al. prepared BT nanoparticles containing reactive thiol groups, which can react with the P(VDF-CTFE-DB) via thiol-ene click reaction[55]. At 450 MV/m, the nanocomposite with 5% BT exhibits an energy density of 11.4 J/cm³, corresponding to a 78% increase compared with the neat polymer, while maintaining a high efficiency of 84.5%.

In addition to nanoparticles, 1D nanowires and nanorods of BT have also been used to improve the energy density of neat fluoropolymers[56–60]. Wang et al. fabricated a nanocomposite composed of BT nanowires and P(VDF-HFP)[58]. The BT nanowires are functionalized with fluoro-polydopamine to increase the affinity to the fluoropolymer matrix. With 5 vol% of BT, a large discharged energy density of 12.87 J/cm³ is measured at 480 MV/m. Recently, alignment of 1D nanorods has been demonstrated to benefit a high energy density at relatively lower electric fields. Xie et al. showed that BT nanowires that are vertically aligned in the

Table 2 Composition, dielectric properties and room-temperature energy storage performance of ferroelectric polymer composites

Polymer	Filler	Young's modulus (MPa)	K @ 1 kHz	tanδ @ 1 kHz	E_b (MV/m)	U_e (J/cm³)	Power density (MW/cm³)	Efficiency (%)	Lifespan (cycles)
0D nanofillers									
PVDF[49]	40 vol.% $BaTiO_3$-PVP		65	<0.02		0.03 @ 10 MV/m			
P(VDF-HFP)[50]	20 vol.% $BaTiO_3$- hydantoin resin		~20	~0.043	330	8.13		56.64	
Crosslinked PVDF[52]	2.0 wt.% $BaTiO_3$-DPA		11.6 (100 Hz)	0.135 (100 Hz)	242	2.9 @ 275 MV/m		75	
PVDF[53]	4 vol.% modified $BaTiO_3$		~11.5	~0.02	517	11.27 @ 520 MV/m		60	
PVDF[54]	50 vol.% modified $BaTiO_3$		~28	0.038	328	9.89		60	
P(VDF-HFP)[79]	10 vol.% SiO_2	986.2	27.1	0.03	390	5.1			
P(VDF-HFP)[128]	0.82 vol.% CdSe/$Cd_{1-x}Zn_xS$	~1500	17.8	0.029	531.6	21.4 @ 531.6 MV/m		78.3	
P(VDF-HFP)[129]	0.8 vol% $Cd_{1-x}Zn_xSe_{1-y}S_y$	~1500	18.6	0.04	621.1	27.4 @ 620 MV/m		70.2	>5×10⁴
1D nanofillers									
PVDF[51]	2.1 vol.% $BaTiO_3$-PDA		~11	<0.04	340.4	7.03 @ 330 MV/m			
P(VDF-HFP)[58]	5 vol.% $BaTiO_3$-PDA		~12	~0.05	~470	12.87 @ 480 MV/m		~55	
P(VDF-CTFE)[59]	3 vol.% Z-aligned $BaTiO_3$		~16		271.9	10.8 @ 240 MV/m		61.4	
PVDF[60]	[110]-$BaTiO_3$		~24	~0.03		11.82 @ 320 MV/m		68.8	

(Continued)

Polymer	Filler	Young's modulus (MPa)	K @ 1 kHz	tanδ @ 1 kHz	E_b (MV/m)	U_e (J/cm³)	Power density (MW/cm³)	Efficiency (%)	Lifespan (cycles)
1D nanofillers									
P(VDF-HFP)[72]	2.37 vol.% $Na_{0.5}Bi_{0.5}TiO_3$		~13	~0.05	458	12.7 @ 458 MV/m			10^6
PVDF[73]	2.1 vol.% $_{0.5}(Ba_{0.7}Ca_{0.3})TiO_3$-$_{0.5}Ba(Zr_{0.2}Ti_{0.8})O_3$		~12	~0.025	374.5	8.23 @ 380 MV/m	2.21	~60	
PVDF[70]	5 vol.% $SrTiO_3$		~12	~0.025	361.2	9.12 @ 360 MV/m	2.31	61.1	
P(VDF-TrFE-CTFE)[68]	TiO_2@PZT		218.9	~0.08	132.4	6.9 @ 143 MV/m		50.0	10^6
P(VDF-HFP[80]	2.5 vol.% TiO_2		~12	~0.04	520	11.13 @ 520 MV/m		60.2	
2D nanofillers									
P(VDF-CTFE)[83]	12 wt.% BNNS+15 wt.% $BaTiO_3$	~750	12	0.036	552	21.2 @ 552 MV/m	0.85	78	
P(VDF-TrFE-CFE)[84]	12 wt. % BNNS	~500		0.027	~600	20.3 @ 650 MV/m		~80	
P(VDF-HFP[81]	5 vol.% Al_2O_3	1600	~10.7	~0.035	697	21.6 @ 700 MV/m	0.96	83.4	$>5\times10^4$
PVDF[85]	BZT-BNNS	2200	16.6 (100 Hz)	~0.05	678.5	23.4 @ 678.5 MV/m		83	
Multicomponent nanofillers									
PVDF[111]	3.6 vol.% $BaTiO_3$@TiO_2@Al_2O_3	~580	~14	~0.02	450	14.84 @ 450 MV/m	4.7	64.5	
PVDF[108]	10 vol.% TiO_2- $BaTiO_3$-TiO_2		12.6	0.05	312.8	4.4 @ 312.8 MV/m		83.3	
P(VDF-HFP)[109]	3 wt.% $BaTiO_3$@MgO	1570	~11	~0.03	571.4	19.0 @ 571.4 MV/m		61.2	
PVDF[110]	1 vol.% $SrTiO_3$@SiO_2		~10	~0.04	402	14.4 @ 402 MV/m		~55	
PVDF[94]	3.6 vol.% $BaTiO_3$@Al_2O_3		~12	~0.02	420.6	10.58 @ 420 MV/m	1.47	63.85	
PVDF[97]	5 wt.% $BaTiO_3$@BNNS	840	~11.5	0.027	610	17.6 @ 580 MV/m		~50	
P(VDF-TrFE-CFE)[98]	BNNS (6 vol.%)-$BaTiO_3$ (3.9 vol.%)		~42	~0.031	527	15.82 @ 530 MV/m	1.08	~75	
P(VDF-HFP)[99]	3 vol.% $BaTiO_3$-$Bi(Li_{0.5}Nb_{0.5})O_3$	2600	~11	0.026	478	14.2 @ 497 MV/m		55.5	$>5\times10^4$
PVDF[100]	2 vol.% $Ba_{0.6}Sr_{0.4}TiO_3$@SiO_2		~14.5	~0.027	525	18.08 @ 525 MV/m		70.06	
Multilayered composites									
PVDF/0.16 vol.% BNNS/PVDF[86]			~11.5	~0.02	612	14.3 @ 612 MV/m	0.069	~70	
PVDF-BNNS/PVDF-BST/PVDF-BNNS[120]			~11.5	~0.022	588	20.5	0.91	~70	
PVDF- $BaTiO_3$[117]			12.5	0.03	390	16.5 @ 390 MV/m		65	
16-layer P(VDF-HFP)-$BaTiO_3$[112]		~1800	~15	~0.04	862.5	30.15 @ 782 MV/m		78	
Gradient P(VDF-HFP)-$BaTiO_3$[118]		1500	~14	~0.04	676.3	18.0 @ 670 MV/m	0.295	~65	
PVDF/PVDF-$K_{0.5}Na_{0.5}NbO_3$/PVDF[122]			~11	<0.05	420	14.2 @ 420 MV/m		78.5	
PVDF/PVDF-$Na_{0.5}Bi_{0.5}TiO_3$/PVDF[123]			~11	~0.03	614.9	30.55 @ 615 MV/m	26.6	80.26	$>2\times10^4$ (bending)
P(VDF-HFP)/Ag@BN/PEI-P(VDF-HFP)[124]			~6	~0.018	510	11.4 @ 510 MV/m	0.165	80	4×10^4
PVDF/P(VDF-TrFE-CTFE)/PVDF[127]			11.11	~0.03	571	18.12 @ 620 MV/m		~50	$>10^6$
P(VDF-HFP)-BT (outer)/PMMA (center)[125]			~5.2	~0.06	559	17.1 @ 559 MV/m		82	>600
PMMA/Al_2O_3-P(VDF–HFP)/P(VDF–HFP)[126]			~11	0.05	600	10.03 @ 600 MV/m		75	$>5\times10^4$
50 vol.% P(VDF-TrFE-CFE)/PI[114]			6.04	~0.022	439.4	9.6 @ ~410 MV/m		58	
PVDF/PMMA[115]			8.38	~0.04	767.05	19.08 @ 767 MV/m		~60	

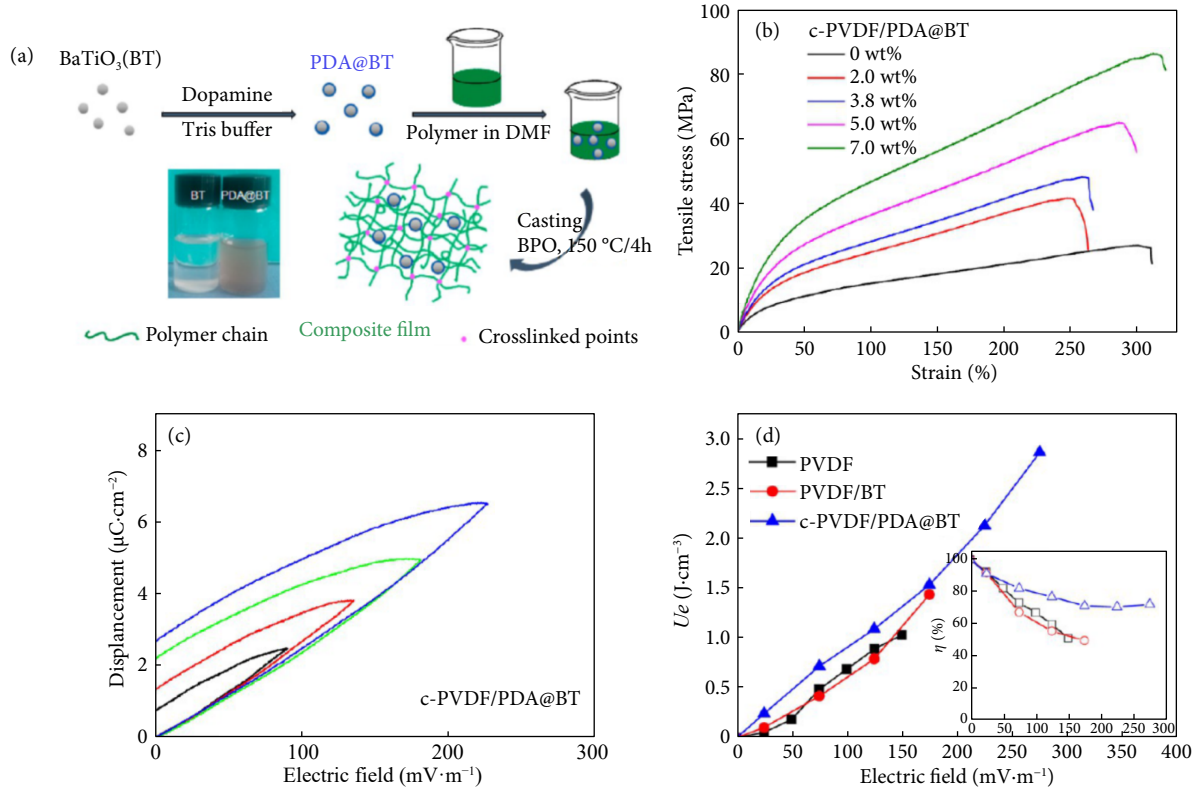

Fig. 2 **(a)** Schematic representation of the synthetic procedures of the PDA@BT nanoparticles and the nanocomposite films. **(b)** Strain-stress curves of c-PVDF/PDA@BT nanocomposites at different BT loading ratios. **(c)** *D-E* loops of *c*-PVDF/PDA@BT nanocomposite with 2.0 wt % nanofiller content. **(d)** Comparison of discharged energy density and efficiency of different materials. Reprinted with permission from Ref. [52], © 2017 American Chemical Society.

P(VDF-CTFE) matrix can generate a higher energy density compared with those aligned in the *X*–*Y* direction[59]. At a relatively low field of 240 MV/m, the composite containing 3 vol% of Z-aligned BT nanowires exhibits an energy density of 10.8 J/cm^3 and an efficiency of 61.4%. In another report, Yao et al. showed that PVDF nanocomposites containing [110]-oriented BT nanorod arrays delivers a high energy density of 11.82 J/cm^3 at 320 MV/m[60].

Other high-*K* ceramics have also been used as nanofillers for improved energy storage performance, such as $Ba_xSr_yTiO_3$ (BST)[61–66], lead zirconate titanate (PZT)[67–68], $SrTiO_3$[69–70], $Ba(Zr_{0.3}Ti_{0.7})O_3$[71], $Na_{0.5}Bi_{0.5}TiO_3$[72], and BCZT[73]. Zhang et al. successfully synthesized highly aligned titanium dioxide/lead zirconate titanate nanowire arrays on the FTO substrate[68]. The P(VDF-TrFE-CTFE)/TiO_2@PZT nanocomposites can be prepared by spin coating of the polymer solution. This nanocomposite exhibits a high energy density of 6.9 J/cm^3 at a low electric field of 143 MV/m, which is attributed to the exceptionally high dielectric constant (K = 218.9 at 1 kHz).

1.2.2 Nanocomposites with oxide nanofillers

In addition to high-*K* ceramics, metal and nonmetal oxides, which often have comparable dielectric constant as the ferroelectric polymers, have been proven to enhance the energy storage performance[74–82]. Li et al. found that ultra-small SiO_2 nanoparticle (0.13 nm) functionalized with perfluorooctyltriethoxysilane (POTS) can significantly improve the dielectric constant of P(VDF-HFP) while maintaining a low dielectric loss, i.e., K = 27.1 and tanδ = 0.03 at 1 kHz[79]. By controlling the grafting ratio of POTS, the perfluorooctyl chains may adopt a polar all-trans conformation while leading to the reduced crystal size of P(VDF-HFP). The energy density is 5.1 J/cm^3 due to the lower breakdown strength with 10 wt% SiO_2 nanoparticles. Although high energy density can be realized in composites containing high-*K* ceramic nanofillers, the efficiency is relatively low, which can be problematic due to the generation of waste heat. Li et al. demonstrated that high energy density (21.6 J/cm^3 at 697 MV/m) and efficiency (83.4% at 700MV/m) can be obtained in P(VDF-HFP)/Al_2O_3 nanoplate composites[81]. A systematic study was conducted to study to effect of dielectric constant, bandgap and morphology of nanofillers on the discharged energy density (Figures 3(a)–3(c)). Three nanomaterials, Al_2O_3 (*K*~10), SiO_2 (*K*~4) and TiO_2 (*K* > 40) are selected to form composites with P(VDF-HFP). Al_2O_3 has a dielectric constant comparable to the polymer matrix, and the dielectrically matching filler/matrix interface leads to a more homogeneous electric field distribution, which translates into a higher breakdown strength. Moreover, the authors discovered that 2D Al_2O_3 nanoplates can form "3D-like" networks in the polymer matrix, which can effectively block the leakage current and at the same time improve the Young's modulus. As shown in Figures 3(d) and 3(e), the P(VDF-HFP)/Al_2O_3 nanoplates composite exhibits a higher breakdown strength and thus a higher energy density than the composite with Al_2O_3 nanoparticles.

1.2.3 Nanocomposites with oxide nanofillers

2D nanofillers, represented by boron nitride nanosheets, BNNSs, have been widely used to reduce the leakage current and improve breakdown strength[83–89]. To improve the dielectric constant, the BNNSs can be used in conjunction with a high-*K* nanofiller such as BT. Li et al. described a simple method to prepare P(VDF-CTFE)/BNNSs/BT ternary composite system[83]. The BNNSs not only suppress the leakage current and reduce the dielectric loss, but also increase the tensile modulus and prevent electromechanical

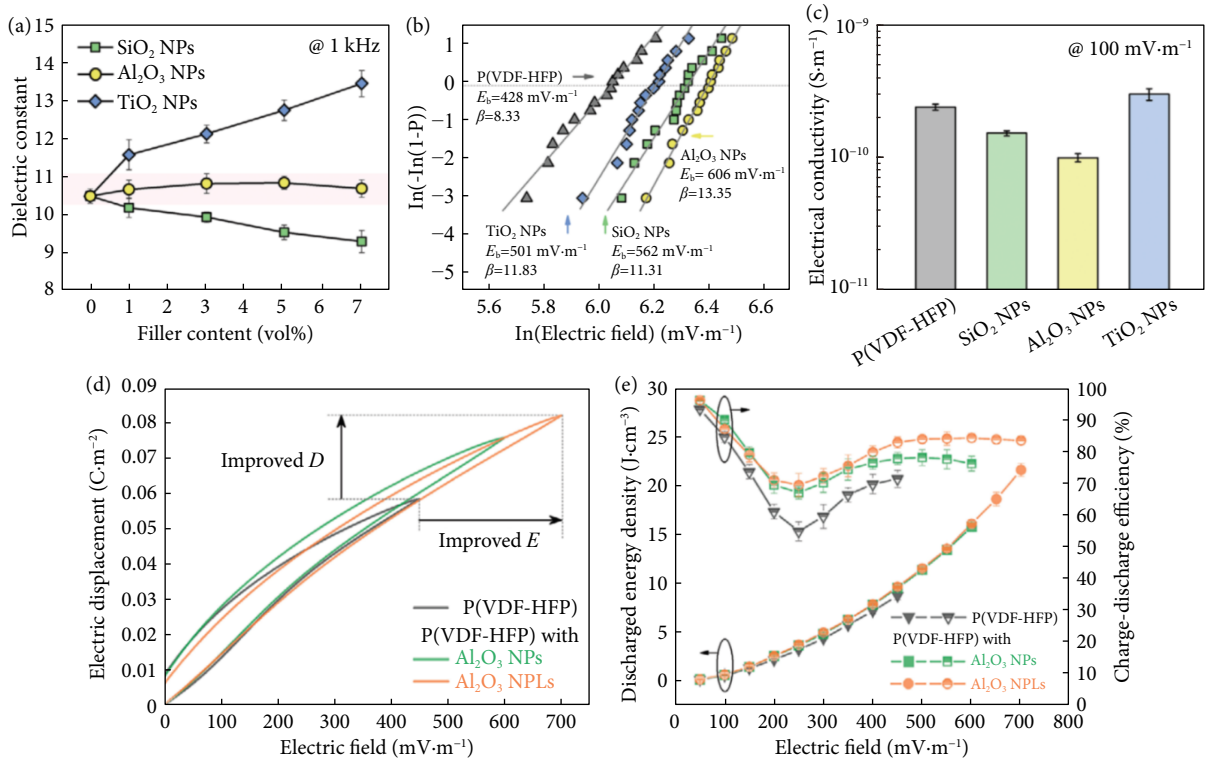

Fig. 3 **(a)** Dielectric constant the P(VDF-HFP) nanocomposites with SiO_2, Al_2O_3, and TiO_2 NPs as a function of filler content. **(b)** Weibull plot of dielectric breakdown strength, and (c) volume electrical conductivity of P(VDF-HFP) and the P(VDF-HFP) nanocomposites with 5 vol% SiO_2, 5 vol% Al_2O_3, and 3 vol% TiO_2 nanoparticles. **(d)** Unipolar *D-E* loops of P(VDF-HFP) and the P(VDF-HFP) nanocomposites with 5 vol% Al_2O_3 nanoparticles and nanoplates. **(e)** Discharged energy density and efficiency of P(VDF-HFP) and the P(VDF-HFP) nanocomposites with 5 vol% Al_2O_3 nanoparticles and nanoplates at varied electric fields. Reprinted with permission from Ref. [81], © 2021 John Wiley and Sons.

breakdown. In the meantime, BT nanoparticles increase the dielectric constant of the base polymer. The synergic effect of two inorganic fillers results in an impressive energy density of 21.2 J/cm³ and a power density of 0.85 MW/cm³. In additional, due to the high thermal conductivity, BNNSs can effectively reduce the heat accumulation in the polymer and reduce the chance of thermal breakdown[84]. With the help of the electrospinning technique, Jiang et al. fabricated P(VDF-HFP)-based composites containing barium zirconate titanate (BZT) and BNNSs with gradient nanofiller concentration. The BNNSs have a reverse concentration gradient as opposed to BZT, and this structure can effectively block the charge injection. A high discharged energy density of 23.4 J/cm³ and an ultrahigh discharge efficiency of 83% are achieved simultaneously. In addition to BNNSs, application of other 2D materials such as graphene and MoS_2 have also been reported[90,91].

1.2.4 Nanocomposites with multicomponent nanofillers

Hybrid and multicomponent nanomaterials have also been developed to improve the energy storage performance of fluoropolymers. BT can be either embedded to or embedded with a range of materials, such as TiO_2, Al_2O_3, Fe_2O_3, SiO_2, Ni, boron nitride (BN), etc[92–100]. For example, Zhang and coworkers prepared $BaTiO_3$@TiO_2 nanofibers where BT nanoparticles (~50 nm in diameter) are dispersed into TiO_2 nanofibers (300 nm in diameter and tens μm in length)[92,93]. The resulted $BaTiO_3$@TiO_2 nanofibers are successfully composited with PVDF and P(VDF-HFP) to deliver giant discharged energy density. Notably, the P(VDF-HFP) containing 3 vol% of hybrid nanofibers displays an energy density of 31.2 J/cm³ at 797.7 MV/m, which is an extremely high electric field for polymer composites[93]. The high breakdown strength is attributed to the orientation of nanofibers which are perpendicular to the external electric field. Li et al. prepared hydroxyl-functionalized BT nanoparticles and phosphonic acid tethered BNNSs, and the hierarchically nanostructured BNNS–BTs can be simply obtained by mixing the two nanomaterials together (Figure 4(a))[98]. At optimal composition and condition, a maximum energy density of 15.82 J/cm³ is measured on P(VDF-TrFE-CFE)/BNNS–BT nanocomposites, outperforming the neat terpolymer and the terpolymer/BT binary composite, as shown in Figure 4(b). Moreover, P(VDF-TrFE-CFE)/BNNS–BT nanocomposite with 6 vol% BNNS and 3.9 vol% BT generated a power density of 1080 MW/L, 10 times higher than that of the BOPP (Figure 4(c)).

Encapsulating the high-*K* BT nanoparticles or nanorods with a shell of another material can significantly mitigate the inhomogeneous interface polarization[101]. Polymers[102,103] and oxides[104–111] are the most used materials for the shell layer. Zhu et al. studied the effect of polymer shell layer on the dielectric and energy storage properties of the composites containing core-shell BT nanoparticles[103]. It is concluded that the breakdown strength of the polymer@$BaTiO_3$-based nanocomposites highly depends on the electrical conductivity of the polymer shell. The nanocomposite with poly(glycidyl methacrylate) shell exhibits the highest energy density of 2.40 J/cm³, although it does not have the highest dielectric constant. This indicates that the discharge energy density depends on both the dielectric constant and breakdown strength. Pan et al. showed that an insulating layer of Al_2O_3 outside the BT nanofibers can effectively reduce the inhomogeneous interfacial polarization and space charge polarization between the fillers and

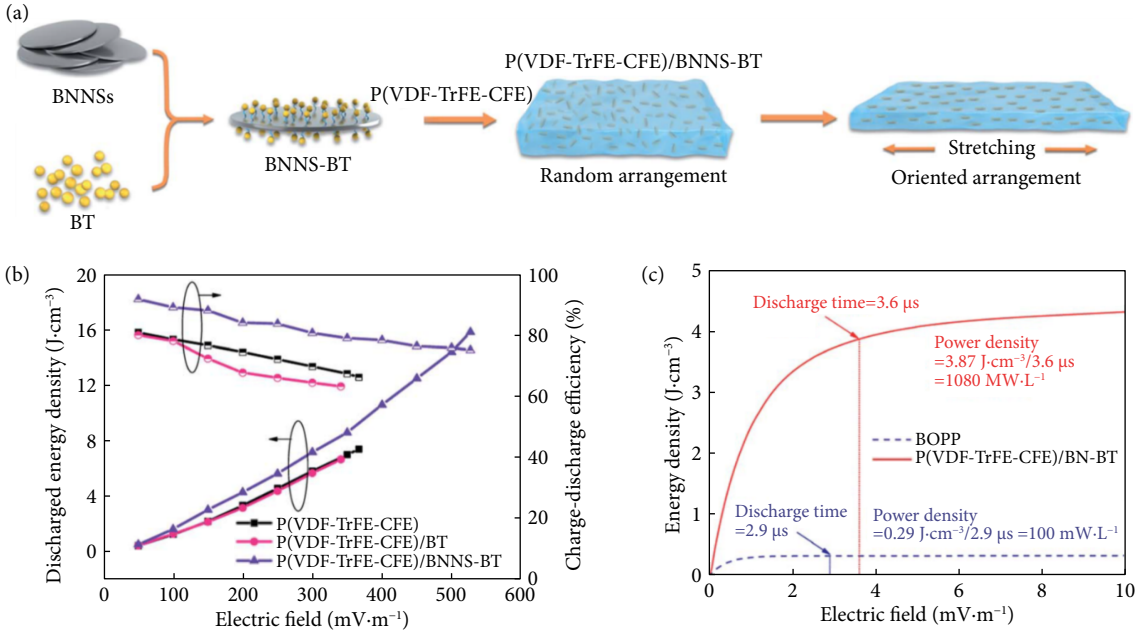

Fig. 4 **(a)** Schematic representation of the synthetic procedures of the P(VDF-TrFE-CFE)@BNNS-BT nanocomposite films. **(b)** Discharged energy density and efficiency of P(VDF-TrFE-CFE), P(VDF-TrFE-CFE)/BT and P(VDF-TrFE-CFE)/BNNS–BT under different electric fields. **(c)** Direct discharged energy density to a 13 kU resistor load as a function of time for BOPP and the P(VDF-TrFE-CFE)/BNNS–BT nanocomposite with 6 vol% BNNS and 3.9 vol% BT. Reprinted with permission from Ref. [98], © 2020 Royal Society of Chemistry.

the polymer matrix[107]. As a result, the PVDF doped with 5 vol% BT@Al_2O_3 exhibits a large energy density of 12.18 J/cm³ at 400 MV/m with an efficiency of 62.5%. Pan et al. designed a core-double shell structured nanofibers denoted as $BaTiO_3$@TiO_2@Al_2O_3[111]. The composite films show a maximum energy density of 14.84 J/cm³ at 450 MV m, along with a high power density (4.7 MW/cm³) and a fast discharging speed of 0.37 μs.

1.2.5 *Layer-structured composites*

In recent years, bilayer and multilayer configuration has been widely adopted to fabricate high-performance nanocomposite for capacitive applications to achieve a very high energy density (35.4 J/cm³)[112]. For example, adding an extra layer of Si_3N_4 or polyimide to the high-*K* polymer film can lead to an improved energy density and efficiency[113–115]. The layered composite films may only contain one type of nanofillers, while the concentration of the nanofiller in each layer is different or even distributed in gradient[116–119]. For instance, Wang et al. designed a nanocomposite film composed of three layers of PVDF/BT films[116]. The middle layer, or the hard layer, contains 1 vol% of BT and works to limit the free electrons and the electrical tree growth. The two outer layers, soft layers, contain high volume ratio of BT nanoparticles (10–50 vol%). The highest energy density (18.8 J/cm³) is obtained in the composite films with 20 vol% BT in the soft layers, which also exhibit a high breakdown strength of 470 MV/m.

A-B-A trilayer structure is another commonly used configuration. The middle layer often works to limit leakage current while the two outer layers provide high dielectric properties[120–125]. Liu et al. fabricated a sandwich-structured composite which is composed of a PVDF/BNNSs middle layer and two PVDF/barium strontium titanate (BST) outer layers, as shown in Figures 5(a)–5(c)[120]. The two BST nanowires embedded outer layers provide high *K* and the middle layer is used to block leakage current. With optimized filler content, this trilayered composite film exhibits a high energy density of 20.5 J/cm³ and a breakdown strength of 588 MV/m. The power density reaches 0.91 MW/cm³, which is nine times of that of BOPP. Sun et al. reported a trilayerd composite film which consists of a Al_2O_3/P(VDF–HFP) middle layer sandwiched between a P(VDF–HFP) and a PMMA layer[126]. An energy density of 10.03 J/cm³ is obtained at 600 MV/m, much higher than that of the bilayer P(VDF–HFP)/PMMA composite. Xie et al. reported an all-organic five-layer composite film composed of alternating PVDF and P(VDF-TrFE-CTFE) films. A high energy density of 18.12 J/cm³ is measured at 620 MV/m[127].

1.2.6 *Composites with ultra-low filler loading*

Although careful design of the nanofiller composition and composite structure can achieve the increase of *K* and E_b at the same time, a relatively high percentage of inorganic filler often yields compromised mechanical properties and processibility. Li et al. reported an unusual discovery that adding < 1% of CdSe/$Cd_{1-x}Zn_xS$ quantum dots (QDs) into P(VDF-HFP) can promote the formation of polar phase in the polymer and thereby increase the dielectric constant of the neat polymer[128]. The wide bandgap of QDs can also suppress the carrier conduction and improve the discharge efficiency. Furthermore, the same author reported that adding < 1 vol% of surfaced modified $Cd_{1-x}Zn_xSe_{1-y}S_y$ (denoted as CZS-APP) nanodots into the P(VDF-HFP) leads to a 100% increase in dielectric constant and 37% increase in breakdown strength compared with the neat copolymer (Figure 6(a))[129]. Consequently, the energy density increases from 6 J/cm³ for the neat copolymer to 27.4 J/cm³ at 600 MV/m for the nanocomposite with only 0.8 vol% of CZS-APP (Figure 6(b)). As shown in Figures 6(c) and 6(d), no other composite systems have achieved such high *K* and U_e at such low loading content. This unexpected increment cannot be explained by the classic composite theory due to the low loading ratio and the similar dielectric constant between the CZS-APP and P(VDF-HFP) (both *K* ~10). Further characterization and simulation reveal that the addition of CZS-

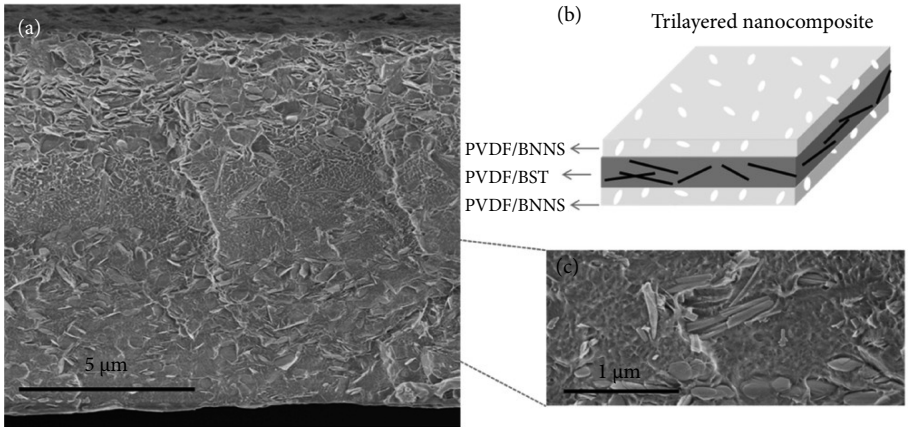

Fig. 5 **(a)** Cross-sectional SEM image of trilayer-structured nanocomposites with 8 vol% BST nanowires in the central layer. **(b)** Schematic of the structure of the trilayered film composed of PVDF/BNNS as outer layers and PVDF/BST as the middle layer. **(c)** SEM image of the interfacial area between PVDF/BNNS and PVDF/BST layers. Reprinted with permission from Ref. [120], © 2017 John Wiley and Sons.

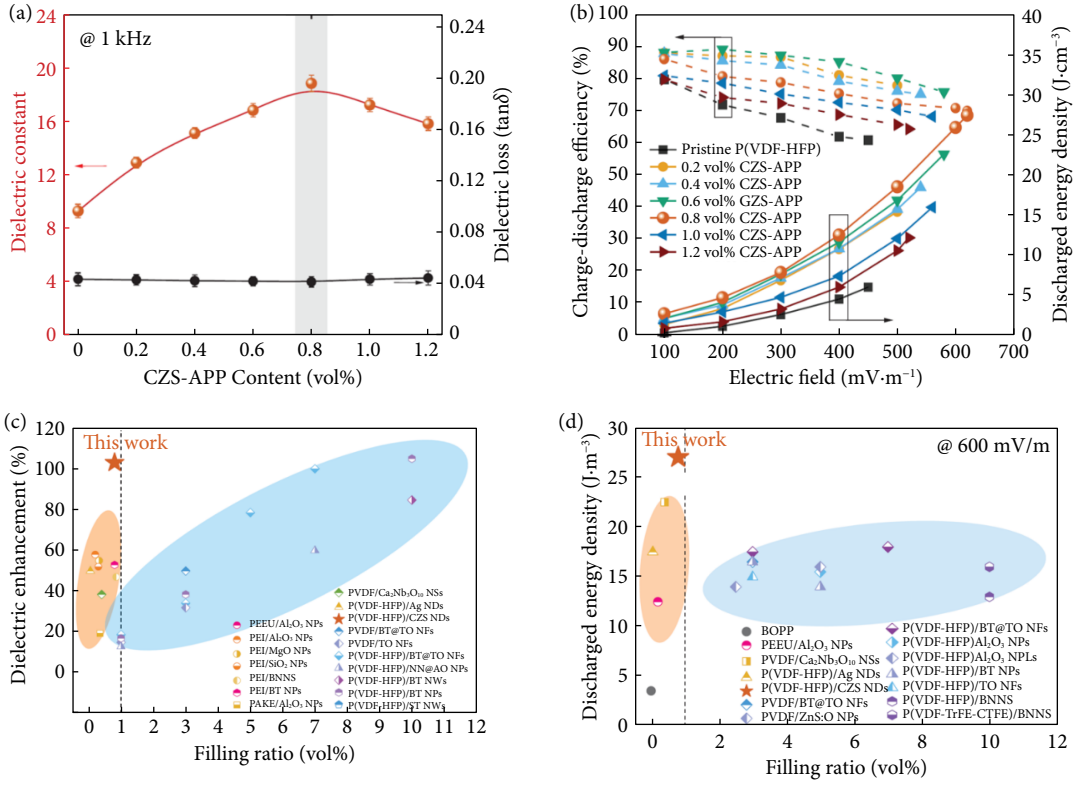

Fig. 6 **(a)** Dielectric constant and dielectric loss **(b)** discharged energy density and efficiency of P(VDF-HFP) and P(VDF-HFP)/CZS-APP nanocomposites as a function of CZS-APP contents. **(c)** and **(d)** show the comparison of dielectric constant enhancement and energy density of this work with previously reported composites. Reprinted with permission from Ref. [129], © 2021 John Wiley and Sons.

APP not only increases the crystallinity of the P(VDF-HFP), but also facilitates the phase transition from the α phase in P(VDF-HFP) to predominant polar β and γ phase in the nanocomposites. The increasing content of polar phase leads to the increase in dielectric constant and polarization, and the presence of γ phase decreases the ferroelectric hysteresis. Additionally, the authors accent the impact of highly polar interface with interfacial dipoles on the high dielectric response of the nanocomposite. The increased breakdown strength is attributed to the increased electrical resistance and improved mechanical modulus.

1.3 All-organic nanocomposites

Small organic molecules have also been added to fluoropolymers to improve the energy storage performance. Rahimabady et al. reported a surprisingly high breakdown strength (868 MV/m) in all-organic films composed of VDF oligomer and poly(vinylidene fluoride) (PVDF)[130]. A maximum polarization of 162 mC/m^2 is obtained since the coexistence of long and short PVDF chains facilitates the dense packing of rigid amorphous phase. This composite displays a high energy density of 27.3 J/cm^3. Zhang et al. showed that adding 0.9 wt% of PCBM into the PMMA/PVDF leads to a high breakdown field of 685.67 MV/m, and thus the energy density reaches 21.89 J/cm^3 with a 70.34% efficiency[131]. The PMMA not only reduce the dielectric loss of PVDF, it is also believed to reduce the free volume and thus the free path of electrons, which explains the high breakdown strength. In addition,

the PCBM at low concentration can capture the free electrons and further reduce the conduction loss.

1.4 Linear dielectric polymers and composites

Linear dielectric polymers typically exhibit much lower dielectric constant than ferroelectric polymers. Nevertheless, they have advantages such as low loss and high efficiency, and rational structural design can lead to significant improvement in their dielectric and energy-storage properties.

Dipolar glass polymers, such as polyimide (PI), represent an important category of polymer dielectrics. Owing to their excellent thermal stability and high glass transition temperature (T_g), they find important applications at high temperature conditions, which will be reviewed in the next section. A number of novel high T_g polymers have been synthesized over the years. Although in some cases the intention is to improve high-temperature energy-storage performance, these polymers do exhibit impressive performance at room temperature[132–138]. Aided by the density functional theory (DFT) computation, a series of polyimide structures were screened for capacitive applications by considering the dielectric constant/loss, bandgap and breakdown strength[132]. Polyimides with high dielectric constant (K = 7.8) and high energy density of 15 J/cm^3 have been discovered. The Zhu group showed that incorporation of highly polar sulfonyl groups (-SO_2) can significantly improve the dielectric constant and energy density of polymethacrylate and poly(2,6-dimethyl-1,4-phenylene oxide) (PPO)[133,134]. Moreover, Zhang et al. reported a novel high-K dipolar glass polymer, denoted as SO_2-PIMs[136]. The intrinsic microporosity in this material provides large free volume for the rotation of dipolar side groups. As a result, an excellent discharged energy density of 17 J/cm^3 is measured at room temperature with an efficiency > 90%. Feng et al. synthesized a block copolymer, polythiourea-*b*-polydimethylsiloxane, PTU-PDMS, and it was observed that the coiled block molecule in the interfacial region can simultaneously induce extra strong charge trapping sites and dipolar polarization[137]. Owing to the low loss, high K as well as the high breakdown strength of 1166 MV/m, this block copolymer exhibits a remarkably high energy density of 29.8 J cm^3.

Composite approach is also used to improve the energy density of linear dielectric polymers[139–142]. Li et al. fabricated bilayered nanocomposite films based on polystyrene[139]. The first layered is doped with wide bandgap Al_2O_3 to reduce the leakage current while the second layered is added with TiO_2 to increase the dielectric constant. This bilayered nanocomposite exhibits a high energy density of 4.43 J/cm^3 under 550 MV/m. Li and coworkers showed that surface modified QDs can significantly improve the K and E_b of PMMA, and thereby a high energy density of 17.6 J/cm^3 and efficiency of > 87% are measured at 800 MV/m[142]. The increase in dielectric constant of the composites is attributed to the formation of interfacial polarization which enhances polymer chain mobility and induces interfacial dipoles. The improved breakdown strength is due to the increased Young's modulus and the high interface charge barriers.

2 Polymers and composites for high-temperature energy storage

There are two major issues concerning the development of high-temperature polymer dielectrics for capacitive applications. First, the polymers should have good thermal stability at elevated temperature without undergoing chemical degradation or thermal transition (glass transition or melting). Linear fluoropolymers and aliphatic polymers are no longer usable at high temperature environment since their melting temperature is generally below 200 °C. For amorphous polymers, a large fluctuation in mechanical and dielectric properties happens when the temperature is in the glass transition range. It should be noted that although the T_g's of PP and PVDF are way below room temperature, their thermal stability is characterized by the melting temperature due to the semicrystalline nature. Therefore, polymers suitable for high temperature applications usually contain rigid aromatic or heterocyclic rings in the polymer backbone with a high T_g, such as polyimide (PI), poly(ether imide) (PEI), fluorene polyester (FPE), cross-linked divinyltetramethyldisiloxanebis(benzocyclobutene) (c-BCB), polycarbonate (PC), poly(phenylene sulfide) (PPS), poly(ether ether ketone) (PEEK) and poly(ether ketone ketone) (PEKK)[10,143–146]. Many of these polymers are commodity engineering polymers that are widely accessible. Although some of these polymers contain polar groups such as ether, imide, or carbonyl groups, their dielectric constants are often much lower (K < 5) than that of the ferroelectric fluoropolymers due to smaller dipole moment and weaker dipole mobility.

Second, leakage current and conduction loss can increase dramatically at high temperature and high electric field[12–13]. While these high T_g polymers exhibit a linear dielectric behavior at room temperature, a poor charge discharge efficiency and degraded breakdown strength are often observed at high temperature even much lower than their T_g. In this regard, the priority of designing high temperature dielectrics is shifted from pursing a very high dielectric constant to limiting conduction loss and retaining high breakdown strength. For convenience, the dielectric properties and high-temperature energy storage performance of recently developed polymers and composites are summarized in Table 3.

2.1 Structural design of high-temperature polymer dielectrics

New high-temperature dielectric polymers have been reported to show improved energy storage performance. Pan et al. synthesized and characterized a new high-temperature polymer, poly(phthalazinone ether ketone) (PPEK)[147]. The hot-press films of PPEK show a stable dielectric constant of 3.5 up to 250 °C. The discharged energy densities reach 2.4 and 2.1 J/cm^3 at 160 and 190 °C, respectively. Zhang et al. showed that poly(2,6-dimethyl-1,4-phenylene oxide) functionalized with small-sized and highly polar methylsulfonyl groups exhibits an enhanced dielectric constant and polarization[134]. Large energy density (up to 22 J/cm^3) and high efficiency (92% at 800 MV/m) are achieved at room temperature. However, the energy density drops to below 2.5 J/cm^3 at 150 °C.

In order to achieve high thermal stability, the base polymers for high temperature capacitive applications often have conjugated aromatic rings in the backbone, at the price of a low bandgap. This may contribute to the high leakage current at high temperature. Wu et al. designed a novel polyolefin structure consisting of repeating units of bicyclic rings and alkenes separated by single bonds[148]. This polymer, named as polyoxafluoronorbornene (POFNB), exhibits a large bandgap of 5 eV. At 150 °C, this polymer exhibits an efficiency > 94% and the maximum energy density reaches 5.7 J/cm^3. Zhang et al. reported a high temperature dipolar polymer based on sulfonylated poly(2,6-dimethyl-1,4-phenylene oxide) (SO_2-PPO). The rotatable methylsulfonyl group gives rise to a large dielectric constant (K~6-8), and the room temperature energy density reaches more than 22 J/cm^3. However, at 150 °C, the material only exhibits an energy density of 2.3 J/cm^3 at 300 MV/m.

Table 3 Composition, dielectric properties and high-temperature energy storage performance of polymer and composite dielectrics

Material	Young's modulus (GPa)	T_g (°C)	K @ 1 kHz*	tanδ @ 1 kHz	E_b (MV/m)	U_e (J/cm³)	Power density (MW/cm³)	Efficiency (%)	Lifespan (cycles)
Poly (phthalazinone ether ketone)[147]		250	3.5	0.0063	441 (190 °C)	2.4 (190 °C)		>70 (<160 °C)	
SO_2-PPO_{25}[134]		211	5.9	0.003 (100 °C)		~2.2 (150 °C)		~80 (150 °C)	
Crosslinked P (CTFE-VDF)[150]			3.19	0.0284	494 (150 °C)	4.33 (150 °C)	0.4 (150 °C)	70 (150 °C)	>5×10⁴
PES-HCuPc coated $BaTiO_3$[152]			~10	~0.04	250 (150 °C)	2.0 (150 °C)		84 (150 °C)	
$BaTiO_3$-BCB@DPAES[155]	~2.7 (rt)		~4.8	0.003	442 (150 °C)	3.1 (150 °C)		~80 (150 °C)	>10⁴
PI-$PbTiO_3$[153]			46	0..023		14 (200 °C)		~79 (200 °C)	
PEI-$SrTiO_3$[154]			~6	<0.04	403.1 (150 °C)	3.18 (150 °C)		~85 (150 °C)	10⁴
c-BCB-BNNS[156]	~2.4 (rt); ~0.6 (250 °C)		3.1	0.001	403 (250 °C)	1.8 (250 °C)		~70 (250 °C)	
h-BN/PEI/*h*-BN[165]			3.1	~0.01		1.19 (200 °C)		~80 (200 °C)	>5.5×10⁴
PEI-$BaTiO_3$-BNNS[164]			3.74	0.00715	547 (150 °C)	2.92 (150 °C)		~70 (150 °C)	>5×10⁴
BN-BCB@DPAES[158]	2.2	206	3.74 (150 °C)	0.006 (150 °C)	547 (150 °C)	4.2 (150 °C)		~85 (150 °C)	>5×10⁴
c-BCB/Al_2O_3 nanoplates[159]	~2.3		~3.5	0.002	482 (200 °C)	3.02 (200 °C)		76.1 (200 °C)	
PI-5 vol.% HfO_2[161]			~3.7	~0.004	397 (150 °C)	2.0 (150 °C)		~70 (150 °C)	>2.5×10⁴
PI-7 vol.% Al_2O_3[161]			~3.6	~0.004	422 (150 °C)	2.1 (150 °C)		~82 (150 °C)	>2.5×10⁴
PEI-Al_2O_3@ZrO_2[163]			3.89	0.004	585 (150 °C)	5.19 (150 °C)		>80 (150 °C)	
PEI-3 vol.%HfO_2[162]			~3.4	~0.004	600 (rt)	2.82 (150 °C)	0.22 (150 °C)	>50 (150 °C)	
PEI-1 vol.% Al_2O_3[178]	~4.1		~3.4	~0.004	503.9 (150 °C)	3.7 (150 °C)		90.1 (150 °C)	
PEEU-0.2 vol.% Al_2O_3[177]			7.4	~0.01	600 (150 °C)	10.6 (150 °C)		~77 (150 °C)	
PEMEU-0.33 vol.% Al_2O_3[176]			7.4	<0.02	500 (150 °C)	2 (150 °C)		90 (150 °C)	
PEI/molecular semiconductors[179]			~3.2	~0.002	~560 (150 °C)	3 (200 °C)		90 (200 °C)	10⁵
c-BCB/BNNS (outer), *c*-BCB/BT (center)[172]			6.3	0.0028	366 (150 °C)	4.0 (250 °C)	0.59 (150 °C)	~80 (250 °C)	>3×10⁴
BN-PI (outer), BZT−BCT (center)[174]			~4	~0.005	350 (150 °C)	1.83 (150 °C)		67 (150 °C)	
SiO_2 deposited polymers[166]						1.24-2.12 (150 °C)		90 (150 °C)	
BN deposited PI[168]			~3.1	~0.001	478 (150 °C)	0.493 (150 °C)		91.3 (150 °C)	
h-BN/PC/*h*-BN[170]			~3	~0.015		3.39 (150 °C)		78.59 (150 °C)	
Al_2O_3-PI-Al_2O_3-PI-Al_2O_3[171]					438.6 (200 °C)	1.59 (200 °C)	0.45 (150 °C)	90 (150 °C)	>5×10⁴
$BaTiO_3$–PEI/BNNS–PEI[173]			7.93	0.021	451.3 (150 °C)	5.4 (150 °C)		90 (150 °C)	>5×10⁴
SiO_2/PEI/SiO_2[167]			~3.1	~0.002	644.5 (150 °C)	2.96 (150 °C)	9.33 (150 °C)	90.16 (150 °C)	>5×10⁴

*The K and tanδ values are measured at room temperature unless noted.

While linear hydrocarbon or fluoropolymer are generally not considered for high temperature applications, crosslinking has been demonstrated to substantially improve their thermal stability and reduce the conduction loss[149,150]. Li and coworkers presented a facile way to fabricate crosslinked P(CTFE-VDF) thin films (denoted as XL-VK)[150]. The preparation procedures and the photograph of the polymer thin film are shown in Figures 7(a) and 7(b). With 3 wt% of dicumyl peroxide as the initiator and 5 wt% of triallyl isocyanurate as the co-agent, the obtained XL-VK-2 exhibits a significantly improve breakdown strength of 494 MV/m at 150 °C (Figure 7(c)), which is even higher than PI and PEI. In addition, an energy density of 2.67 J/cm³ and efficiency of 90% are measured at 150 °C and 400 MV/m (Figure 7(d)). As shown in Figure 7(e), the XL-VK-2 outperforms the reported high-temperature dielectric polymers and composites in terms of the energy density at 150 °C, with a maximum U_e of 4.33 J/cm³ obtained at 526 MV/m.

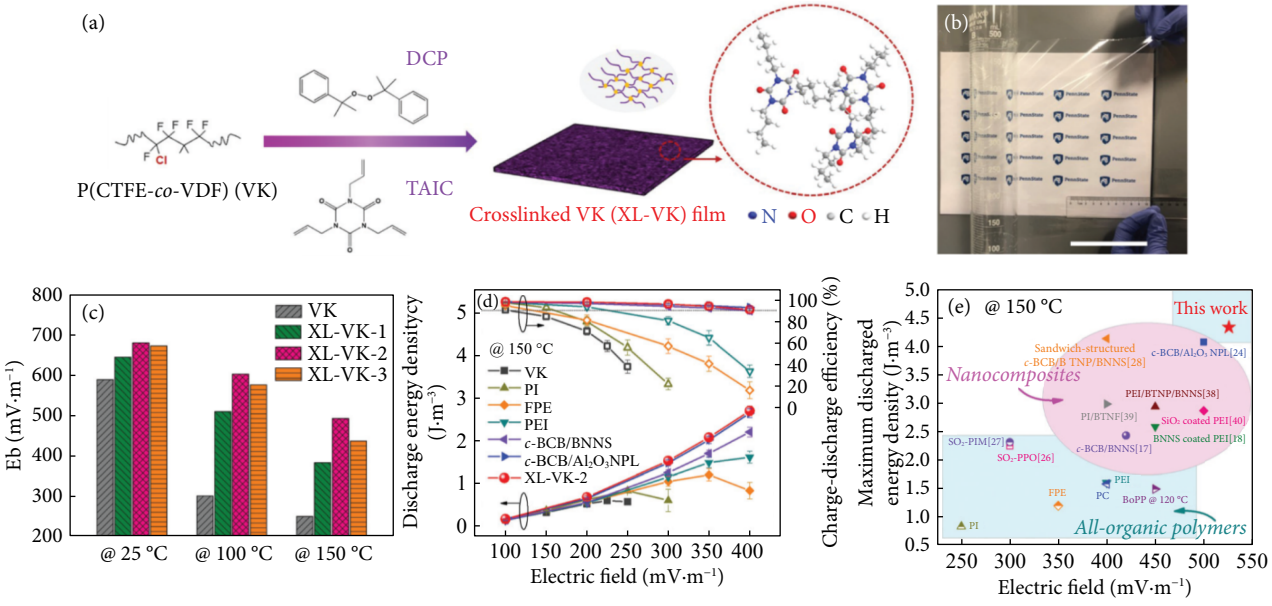

Fig. 7 **(a)** Schematic of the preparation procedures of crosslinked VK (XL-VK) films. **(b)** Photograph of a 12 mm-thick XL-VK-2 film wrapped on a 500 mL graduated cylinder (scale bar: 10 cm). **(c)** Weibull breakdown strength of pristine VK and XL-VK measured at 25, 100 and 150 °C, respectively. XL-VK-1, -2, and -3 are prepared with 2, 3 and 4 wt% dicumyl peroxide initiator, respectively. **(d)** Discharged energy density and efficiency of XL-VK and other high temperature dielectrics at 150 °C under various electric fields. **(e)**. Comparison of the maximum discharged energy density of high-temperature dielectric polymers and composites at 150 °C. Reprinted with permission from Ref. [150], © 2020 Royal Society of Chemistry.

2.2 Composites of high T_g polymers

Forming nanocomposite with high T_g polymers remains the most visited method to suppress the conduction loss and improve the breakdown strength of high T_g polymers at elevated temperature. Despite a few reports to use high-*K* nanofillers to increase the dielectric constant, most studies focus on the reduction of electrical conduction and improvement on the breakdown strength.

2.2.1 Composites with high-K nanofillers

Like room temperature dielectric composites, high-*K* inorganic fillers such as BT have been also been composited with high T_g dielectric polymers in an attempt to improve their dielectric constant and hence the energy density. Sun et al. observed the increase of room temperature dielectric constant from 3.1 to 6.8 after adding 9 vol% BT nanoparticles into neat PI[151]. However, due to the large difference of dielectric constant between the BT and PI as well as the poor thermal conduction of PI, the composite film exhibits much lower breakdown strength at >150 °C even with 1 vol% BT. As a result, the simple PI/BT nanocomposites actually show inferior discharged energy density than the neat PI. This study stresses the significance of conduction loss and breakdown strength at elevated temperature. Xu et al. synthesized a type of hyperbranched phthalocyanine (HCuPc) as a coating layer on the BT nanoparticles[152]. The aryl-SO_2-aryl units are introduced to block the electrical conduction of CuPC. Compared with unmodified BT and CuPC/BT, the HCuPC can evidently lower the dielectric loss and increase the breakdown strength of the composite. The HCuPc/poly(ether sulfone) (PES) composite exhibits a discharged energy density of 2.0 J/cm³ at room temperature and 300 MV/m, while the value is only 1.2 J/cm³ for the neat polymer at the same condition. Jian et al. fabricated a thermally stable composite composed of PI and tetragonal $PbTiO_3$ nanofibers[153]. Impressively, at a high loading ratio of 50 vol% $PbTiO_3$, the composite shows a discharge energy density of 14 J/cm³ at 200 °C and 300 MV/m, slightly decreasing from the room temperature value of 16 J/cm³. In comparison, the energy density of PI is only 1.38 J/cm³. Miao et al. reported another PEI composite containing 5 vol% $SrTiO_3$ nanoparticles to improve the heat dissipation[154]. The composite exhibits an energy density of 6.6 J/cm³ at 100 °C and 3.18 J/cm³ at 150 °C.

To resolve the dielectric loss and leakage current issues from the interface between the BT and polymer matrix, Liu et al. designed a dual crosslinked network denoted as BT-BCB@DPAES[155]. The matrix polymer, DPAES, is based on the structure of poly(arylene ether sulfone) with pendent reactive carbon-carbon double bonds. Since BT nanoparticles is surface functionalized with bisbenzocyclobutene (BCB) groups, the BT-BCB nanofillers can be chemically bonded to the DPAES via Diels–Alder reaction. Compared with non-crosslinked and single-crosslinked composite, the dual crosslinked composite exhibits the highest breakdown strength of 442 MV/m at 150 °C. The maximum energy density reaches 3.1 J/cm³ at 400 MV/m with an efficiency of 75.6%.

2.2.2 Composites with wide bandgap nanofillers

As discussed in previous section, the low energy density at high temperature mainly comes from the low efficiency due to conduction loss and degraded breakdown performance. Wide bandgap nanofillers with moderate dielectric have been demonstrated to significantly improve the charge-discharge efficiency and breakdown strength of high T_g polymers at elevated temperature.

Boron nitride nanosheet, or BNNSs, is a type of wide bandgap (~6 eV) 2D materials with excellent thermal conductivity. In 2015, Li et al. reported that incorporation of BNNSs into *c*-BCB matrix can significantly reduce its electrical conduction and maintain a high breakdown strength at temperatures above 150 °C[156]. At that time, this composite sets a record high energy density of 2 J/cm³ at 200 °C and 1.8 J/cm³ at 250 °C, surpassing all other commodity high T_g polymers. The nanocomposite exhibited an impressively

high Weibull breakdown strength of 403 MV/m at 250 °C and an efficiency > 90% at 150 °C up to 400 MV/m. The simulation confirms that reduced conduction current and high thermal conductivity of BNNSs prevent the overheating and thermal runaway in localized area in the composite films. The suppressed leakage current has also been reported in PI films containing boron nitride interlayer[157]. The PI/BNNSs composite films exhibit an energy density of 2.58 J/cm^3 and an efficiency of 90% at 150 °C. Inspired by the composite structure of natural spider silk, Xu et al. prepared a type of nanocomposite in which the *c*-BCB/BNNSs is chemically bonded with the poly (aryl ether sulfone) (DPAES) via Diels–Alder reaction[158]. The multiple chemical bonding between the filler and the polymers creates a nanoconfinement effect, which not only improves the Young's modulus of this composite, but also freezes the polymer chain motion and reduce charge hopping at high electric field. The BN-BCB@DPAES nanocomposite exhibits a high breakdown strength of 547 MV/m at 150 °C. Meanwhile, the composite with 10 vol% filler exhibits a maximum energy density of 4.2 J/cm^3 at 500 MV/m and maintains an efficiency > 90% at 400 MV/m.

Since *c*-BCB is a rather expensive specialty polymer and the synthesis of BNNSs involves cumbersome solution-phase exfoliation process that is difficult to scale up. Composites made from easily obtained nanofillers and commodity polymers are important for practical applications. Li et al. studied the effect of morphology of γ-Al_2O_3 on the energy storage performance on the *c*-BCB/γ-Al_2O_3 nanocomposite[159]. Compared with BNNSs, γ-Al_2O_3 has a larger bandgap (7.2–8.8 eV vs. 6 eV) a higher dielectric constant (9–10 vs. 3–4). Three types of γ-Al_2O_3 nanofillers have been mixed with the *c*-BCB matrix, including nanoparticles (~20 nm in diameter), nanowires (~5 nm in diameter & ~80 nm in length), and hexagonal-shaped nanoplates (~30 nm in thickness & 800–1000 nm in width). Interestingly, the nanoplates are more effective in improving the breakdown strength of the composites, as the simulation suggests that nanoplates better prevent the inhomogeneous distribution of local electric fields. The benefit of high aspect ratio has been previously demonstrated on fluorene polyester (PES) composite containing titanium phenyl phosphonate nanoplatelets[160]. As showed in Figures 8(a)–8(d), the *c*-BCB composite with 7.5 vol% γ-Al2O3 nanoplates delivers an energy density of 4.07 J/cm^3 at 150 °C while maintaining an efficiency over 90% at 450 MV/m.

A systematic study by Ai and coworkers further confirms the importance of bandgap of nanofillers on the high temperature performance of dielectric composites[161]. Four types of nanofillers with varied dielectric constants and bandgaps, including Al_2O_3, TiO_2, HfO_2 and BNNSs, are composited with PI via in situ polycondensation at the presence of nanofillers. Although PI/TiO_2 composite exhibits the highest room temperature dielectric constant, its shows poorer energy density compared with other nanocomposites due to the smallest bandgap of TiO_2 among four nanofillers. At 150 °C and 250 MV/m, the energy density and efficiency are measured to be 1.12 J/cm^3 and 93.7% for PI/Al_2O_3, and 1.21 J/cm^3 and 91.0% for PI/HfO_2 composite. This work reaffirms the large bandgap nanofillers with moderate dielectric constant can effectively block the conduction current by increasing the trapped depth, which is eventually reflected by the evidently improved efficiency and breakdown strength. In another report, HfO_2 is dispersed into PEI via sonication followed by solution casting[162]. At 150 °C, a maximum energy density of 2.82 J/cm^3 is

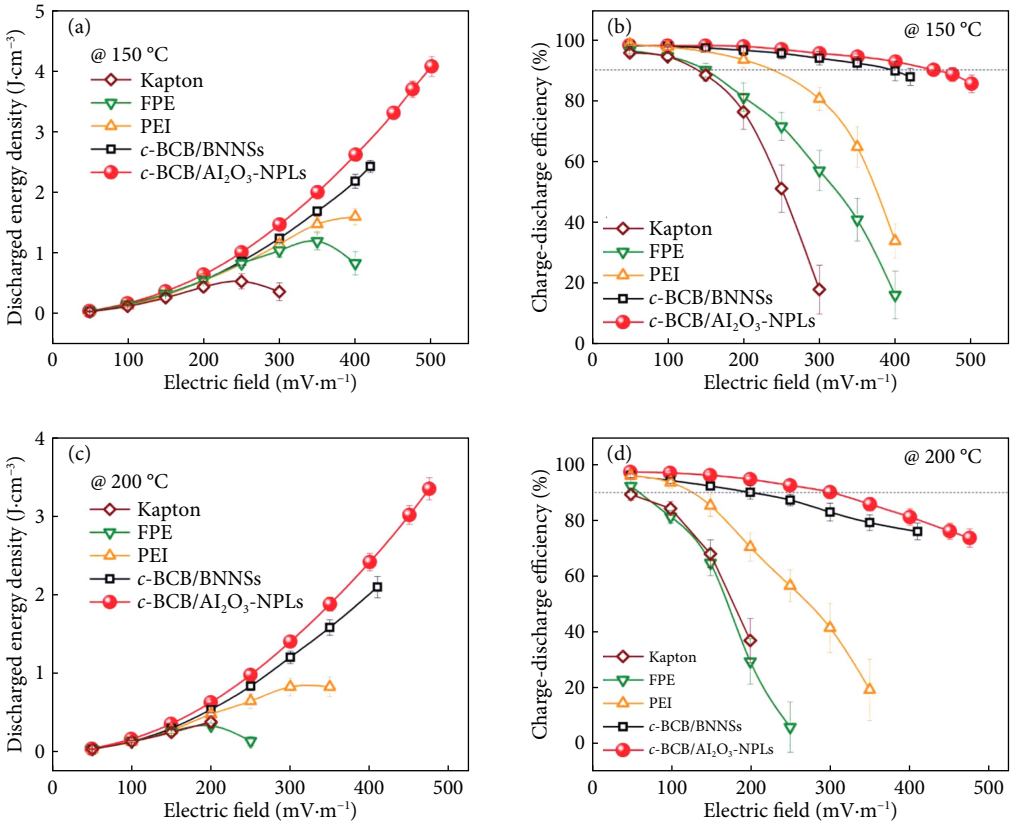

Fig. 8 Comparison of discharged energy density and charge-discharge efficiency of high-temperature dielectric polymers and the c-BCB nanocomposites measured at 150 °C **(a,b)** and 200 °C **(c,d)**. The c-BCB/BNNs composite contains 10 vol% BNNSs and the c-BCB/Al_2O_3 composite contains 7.5 vol% Al_2O_3 nanoplates. Reprinted with permission from Ref. [159], © 2019 John Wiley and Sons.

measured on PEI/HfO_2 with 3 vol% HfO_2, at 500 MV/m. Besides, the nanocomposite also shows a higher power density (0.22 MV/cm^3 vs 0.18 MV/cm^3) than the neat PEI.

Hybrid nanofillers have also been synthesized and used as nanofillers. Ren et al. designed a type of core-shell structured nanocomposite in which high dielectric constant ZrO_2 (K~25) core is encapsulated by high bandgap Al_2O_3 (K~8–10) shell[163]. When incorporated into the PEI, the core-shell structure creates a gradient dielectric constant and thus alleviates the distortion of the electric field around the nanoparticles. At optimized nanofiller content of 11 vol%, the PEI/Al_2O_3@ZrO_2 nanocomposite exhibits a high breakdown strength of 585 MV/m at 150 °C. Due to the enhanced displacement and reduced conduction loss, this nanocomposite displays an energy density of 3.11 J/cm^3 and an efficiency of 92.6% at 150 °C and 400 MV/m, while the values are 2.96 J/cm^3 and 88.0% for PEI/ZrO_2. Li et al. reported a ternary composite consisting of high-K BT nanoparticles, BNNNs and PEI[164]. The synergetic effect of two complementary nanofillers enables the composite films to generate a high energy density of 2.92 J/cm^3 and breakdown strength of 547 MV/m.

2.2.3 *Layer-structured composites*

In addition to homogenous nanocomposites, hierarchical structures, such as layered structures, have also been introduced to improve the energy storage capability of high-temperature dielectric polymers. For example, deposition of ~100 nm of inorganic material on both side of the polymer substrate like a coating layer has attracted much interest. In lieu of dispersing BNNSs into the *c*-BCB matrix, Azizi reported a scalable method to produce hexagonal BN (*h*-BN) films to deposit *h*-BN on Cu foils via low-pressure chemical vapor deposition (CVD)[165]. The *h* -BN films were then transferred onto the PEI films by hot press followed by chemical etching of Cu substrates. While *h*-BN coating has a negligible effect on the low-field dielectric properties of the PEI films, an effective electron barrier is generated between the *h*-BN/PEI and the electrodes owing to the large bandgap of *h*-BN, which effectively blocks the charge injection and thus reduces the dielectric loss. At 200 °C, the sandwiched structured *h*-BN/PEI/*h*-BN films have a more distinct advantage and generate an energy density of 1.19 J/cm^3, more than two times of that of the *c*-BCB/BNNS. Besides BN, SiO_2 was successfully deposited on a variety of polymer substrates[166,167]. Zhou et al. reported a plasma-enhanced chemical vapor deposition (PECVD) process which is also compatible with roll-to-roll manufacturing and promising for scale-up production[166]. The BOPP-SiO_2 composite made from this method exhibits a much improved energy density (1.33 J/cm^3) at 120 °C, a temperature at which pristine BOPP capacitors can barely work. Moreover, this method can be expanded to form composite with other high T_g polymer substrates. PEI-SiO_2 exhibits the highest energy density of 2.12 J/cm^3 and an efficiency > 90% at 150 °C. The SiO_2 layer can withstand more than 50000 charging/discharging cycles without degradation.

Sandwich structured BN/PI/BN composite films were fabricated by direct magnetron sputtering of BN onto the PI surface[168]. With an optimal BN thickness of 142 nm, the BN/PI/BN composite exhibits a breakdown strength of 478 MV/m. At 150 °C and 200 MV/m, the composite film shows an energy density of 0.492 J/cm^3 along with an efficiency of 91.3%, compared with the efficiency of 72.7% for neat PI. In another work, the same group utilized three different techniques, magnetron sputtering (MS), atom layer deposition (ALD) and electron beam evaporation (EBE), to deposit SiO_2, HfO_2, Al_2O_3 and TiO_2, respectively, onto the PEI films[169]. At the optimal condition, all composite films have a better energy storage performance than the neat PEI. The comparison study shows that PEI coated with Al_2O_3 delivers the highest energy density (i.e., 2.8 J/cm^3 @ 90% efficiency at 200 °C), implying that well-balanced bandgap, dielectric constant, and electrical conductivity values are desired. By means of electrospinning and hot pressing, Liu et al. fabricated *h*-BN/PC/*h*-BN composite films, which exhibit an energy density of 3.39 J/cm^3 and efficiency of 78.6% at 150 °C[170].

Dong et al. reported a multilayer composite whose structure can be represented as *X*-PI-*X*-PI-*X*, where *X* is one of the three metal oxides, Al_2O_3, ZrO_2 or MgO[171]. It is found that the composite with Al_2O_3 exhibits an ultra-high energy density, i.e., 2.74 J/cm^3 at 150 °C and 1.59 J/cm^3 at 200 °C, both with the efficiency ≥ 90%. The three layers of Al_2O_3 are more effective to block the leakage current and charge transport than the conventional tri-layered composite. Other configurations, such as those containing multiple layers with different nanofillers, have also been reported[172–174]. To address the low dielectric constant of *c*-BCB/BNNSs composite, a sandwich-structured composite was proposed with a layer of *c*-BCB/BT to increase the dielectric constant between two layers of *c*-BCB/BNNSs[172]. With 25 vol% of BT nanoparticles, the sandwiched-structured nanocomposite delivers a discharged energy density of 1.1 J/cm^3 and an efficiency of 93% at 150 °C and 200 MV/m, outperforming the *c*-BCB/BNNS/BT single layer nanocomposite. Moreover, the power density of the nanocomposite remains about 585 MW/L at temperature up to 150 °C.

2.2.4 *Composites with ultra-low filler content*

In 2017, Thakur et al. discovered an unconventional phenomenon that multiple nanoparticles, in spite of different chemical composition, can significantly increase the dielectric constant of PEI at very low loading ratio[175]. Inspired by this result, the low loading ratio approach has since been used to improve the high temperature capacitive performance of various composite systems[176–178]. Zhang et al. discovered that 0.21 vol% of Al_2O_3 in poly(arylene ether urea) (PEEU) can concurrently increase the room temperature dielectric constant from 4.7 to 7.4 (Figure 9(a)), and the breakdown strength from 600 to 900 MV/m (Figure 9(b))[177]. As indicated by the FTIR data, the enhancement of dielectric response is attributed to the disruption of hydrogen bonding and thus generation of free volume dipoles in PEEU as a result of addition of small amount of Al_2O_3. Besides, crystal structure analysis indicates a slight increase in crystallinity and reduced crystal sizes. This may result in a shorter mean free path for mobile electrons in the composite, which is beneficial to the high breakdown strength. At 150 °C, this composite exhibits a remarkably high energy density of 5 J/cm^3 at 90% efficiency, and a maximum energy density reaches 10.6 J/cm^3 at 600 MV/m (Figures 9(c)–9(e)). It should be noted that this composite also delivers an ultra-high room temperature energy density of 27 J/cm^3 at 900 MV/m, comparable to the best ferroelectric composites. Similar enhancement has also been reported in composites with PEI and poly(ether methyl ether urea) (PEMEU) as base polymers[176,178].

2.2.5 *Composites with ultra-low filler content*

While most composites almost exclusively contain inorganic nanofillers, Yuan et al. pursed an fundamentally different approach to improve the energy storage performance of PEI by adding high-electron-affinity molecular semiconductors, such as ITIC, PCBM and DPDI[179]. The justification of this method is that these semi-

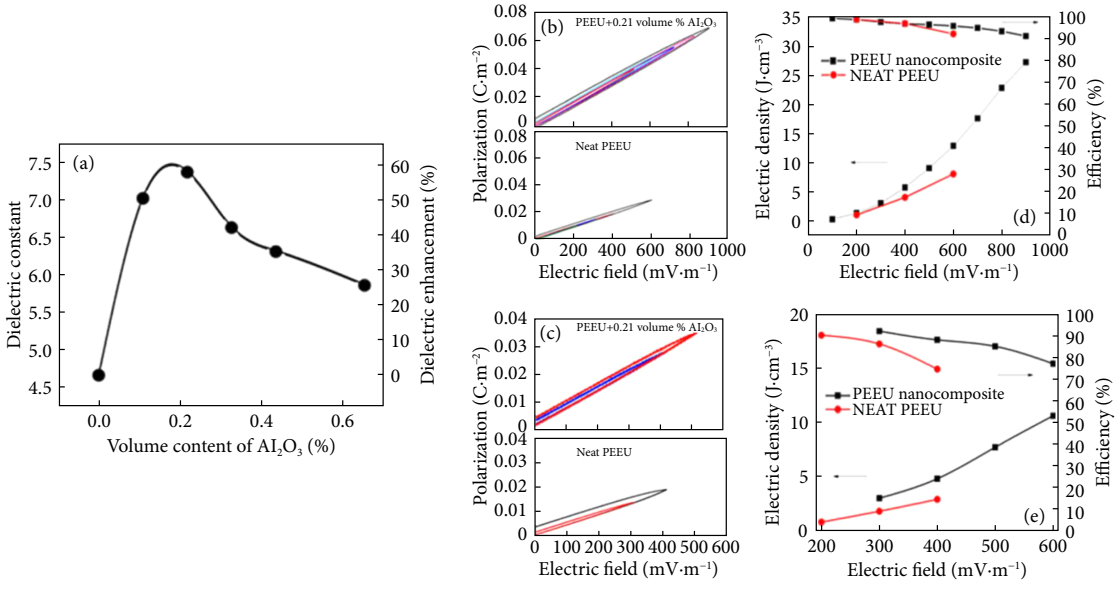

Fig. 9 **(a)** Dielectric constant of PEEU/Al2O3 nanocomposite as a function of Al_2O_3 volume content. **(b)** and **(c)** show the D-E loops of neat PEEU and PEEU/Al_2O_3 nanocomposite at room temperature and 150 °C, respectively. **(d)** and **(e)** show the discharged energy density and efficiency of neat PEEU and PEEU/Al_2O_3 nanocomposite at room temperature and 150 °C, respectively. Reprinted with permission from Ref. [177], © 2020 American Association for the Advancement of Science.

conducting molecules can effectively capture the ejected free electrons as long as the these molecules are thermally stable and their concentration is below the percolation threshold. Indeed, at 200 MV/m and 200 °C, the electrical resistivity of PEI/PCBM is two orders of magnitude higher than the neat PEI. As a result, these composites can maintain a remarkably high efficiency (> 90%) even at 200 °C and 400 MV/m (Figures 10(a) and 10(b)). As shown in Figure 10(c), the energy density above 90% efficiency reaches 3.0 J/cm^3 for PEI/PCBM composite at 200 °C, more than two time higher than previously reported nanocomposites at the same condition. Furthermore, this method is also effective in other polymer systems such as polyethersulfone (PES), fluorine polyester (FPE) and polyimide (PI).

2.3 Other high-temperature dielectrics

Polytetrafluoroethylene (PTFE) is known for its high thermal stability and high-temperature applications. Luo et al. reported thin PTFP films (< 5 μm) can be made from spin-coating of PTFE nanoparticles followed by heat-treatment. The resulted PTFE films exhibit an energy density of 1.08 J/cm^3 and a power density of 0.72 MW/cm^3 with a fast discharge time (~2.95 μs)[180]. Furthermore, the PTFE films coated with epoxy generate an energy density of 1.93 J/cm^3 at 150 °C[181]. There are a number of other reports on high-temperature polymer and composite dielectrics, although their properties are often characterized at temperature below 150 °C[182–186]. For example, Zhou et al. reported that the working temperature of PP can be increased to 120 °C by adding MgO nanoparticles[185]. The MgO nanoparticles are surfaced-modified with polypropylene-graft-maleic anhydride so that the nanoparticles can form homogenous composite with the PP matrix without aggregation. This composite generates an energy density of 1.66 J/cm^3 while maintaining an efficiency of 90% under 400 MV/m at 120 °C.

3 Conclusion and outlook

Here, we review the major strategies to improve the capacitive performance of polymer dielectrics and composites from a material point of view. Many new materials have emerged to show promises as a better alternative to current commercial products, which will benefit the development of more efficient and sustainable electrical systems. Ideally, simultaneous increase in dielectric constant, breakdown strength and charge-discharge efficiency can maximize energy-storage performance of the dielectric materials for both room temperature and high temperature applications. High dielectric constant can be realized either by the discovery of new polymers, modification of existing polymers, or by forming composites with high-*K* nanofillers. The breakdown strength can be increased by the improved thermal conductivity, reduced dielectric/conduction loss and enhanced Young's modulus. Reducing the conduction loss is critical to the high charge-discharge efficiency, and large bandgap nanofillers are shown to effectively block the leakage current and suppress the conduction loss. Moreover, the configuration of dielectric films has evolved from a single-layered structure to multilayered and hierarchical structures. Integration of different approaches can produce a synergistic effect to further enhance the capacitive performance of the dielectric polymers and composites.

There are also challenges to be tackled in the future. There is still room for further improvement of discharged energy density, especially at high temperature. High energy density (~30 J/cm^3) has been achieved in several polymer and composite systems at room temperature, which is comparable to the energy density of supercapacitors. However, these values are often obtained near the breakdown electric field, and packaged capacitors are unlikely to operate at such high electric field for reliability concerns. At high temperature such as 150 °C or above, the energy density can hardly exceed 5 J/cm^3. Further improvement may need a more intricate material design and further understanding on the dielectric behavior of materials at various temperatures and electric fields. In addition to the commonly reported parameters, other factors such as mechanical properties, scalability, processibility and long-term reliability should also be considered for practical applications. Most recently, the self-healing behavior of dielectrics has drawn much attention as it is crucial to the lifetime and reliability of dielectric materials in the real-world applications[187].

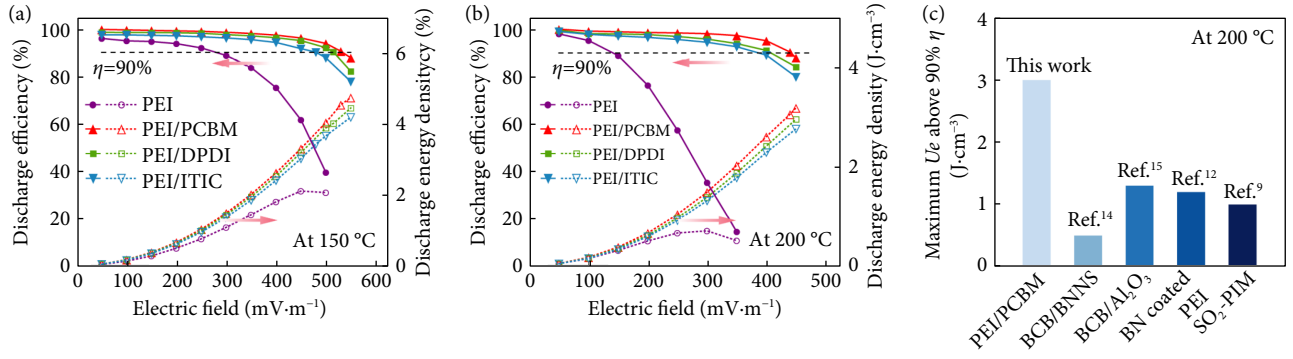

Fig. 10 **(a)** and **(b)** show the discharged energy density and efficiency of PEI neat polymer, PEI/PCBM (0.5 vol.% PCBM), PEI/DPDI (0.75 vol.% DPDI), and PEI/ITIC (0.25 vol.% ITIC) composites, at 150 and 200 °C, respectively. **(c)** Comparison of maximum discharged energy density at above 90% efficiency between the PEI/PCBM and other polymer-based high-temperature dielectrics at 200 °C. Reprinted with permission from Ref. [179], © 2020 Springer Nature.

Polymer-based nanocomposites constitute a large fraction of high-performance dielectrics and they often exhibit superior energy-storage performance than pristine polymers. It is widely accepted that the nanofiller-polymer interface plays a profound role in the properties of nanocomposites. However, despite the various models and theories, it still lacks direct characterization and imaging methods to probe the properties of this interface area to validate these hypotheses. Recently, Yang and coworkers used atomic force microscopy–infrared spectroscopy (AFM–IR) to directly map the polymer chain conformation in P(VDF-TrFE-CFE)/BT nanocomposite[188]. The results indicate that the interfacial coupling in the composite is rather inhomogeneous, and largest interfacial coupling occurs much farther than the bonded layer predicted by multicore model. Similar researches are expected in the future to further elucidate how the nanofillers can lead to the property changes in the nanocomposites.

In addition, most of the literature reports in this topic mainly focus on the materials development. More demonstrations of polymer/composite-based dielectric capacitors in practical applications are needed, such as in portable devices, flexible electronics, electrical power systems and etc. Integration of these new materials into working devices needs more stringent testing of the reliability of the materials as well as considerable engineering innovations. The capability for scale-up production is another important issue for real-world applications. Many reported high-performance dielectric films are prepared in small sizes by laboratory-scale techniques such as solution casting and layer-by-layer deposition. For polymer composite dielectrics, the inhomogeneous dispersion of fillers and interfacial polarization should be addressed in large-scale production. Many programs have been initiated across the industry to improve the scalability of the dielectric films for capacitors, and more progress is expected in the future[189].

Traditionally, the development of new materials relies heavily on the intuition and scientific acumen of the researchers based on the understanding of material properties and previous results. Rational material design aided by simulation and machine learning may provide a more efficient and guided platform for the search of new materials. For example, Ramprasad and coworkers have successfully demonstrated the application of DFT and genetic algorithm can be used to predict polymers with high energy-storage potential[190–192]. The future development of high-performance polymer dielectrics will require interdisciplinary efforts from chemistry, solid state physics, material characterization, electrical engineering and advanced computation techniques.

Article history

Received: 19 December 2021; Revised: 12 March 2022; Accepted: 13 March 2022

Additional information

Declaration of competing interest

The authors have no competing interests to declare that are relevant to the content of this article.

References

[1] Sarjeant, W. J., Zirnheld. J., MacDougall, F. W. (1998). Capacitors. *IEEE Transactions on Plasma Science*, 26: 1368–1392.

[2] Christen, T., Carlen, M. W. (2000). Theory of ragone plots. *Journal of Power Sources*, 91: 210–216.

[3] Sarjeant, W. J., Clelland, I. W., Price, R. A. (2001). Capacitive components for power electronics. *Proceedings of the IEEE*, 89: 846–855.

[4] Johnson, R. W., Evans, J. L., Jacobsen, P., Thompson, J. R., Christopher, M. (2004). The changing automotive environment: High-temperature electronics. *IEEE Transactions on Electronics Packaging Manufacturing*, 27: 164–176.

[5] Wang, Y., Zhou, X., Chen, Q., Chu, B. J., Zhang, Q. M. (2010). Recent development of high energy density polymers for dielectric capacitors. *IEEE Transactions on Dielectrics and Electrical Insulation*, 17: 1036–1042.

[6] Zhu, L., Wang, Q. (2012). Novel ferroelectric polymers for high energy density and low loss dielectrics. *Macromolecules* , 45: 2937–2954.

[7] Chen, Q., Shen, Y., Zhang, S. H., Zhang, Q. M. (2015). Polymer-based dielectrics with high energy storage density. *Annual Review of Materials Research*, 45: 433–458.

[8] Li, Q., Wang, Q. (2016). Ferroelectric polymers and their energy-related applications. *Macromolecular Chemistry and Physics*, 217: 1228–1244.

[9] Li, H., Liu, F. H., Fan, B. Y., Ai, D., Peng, Z. R., Wang, Q. (2018). Nanostructured ferroelectric-polymer composites for capacitive energy storage. *Small Methods*, 2: 1700399.

[10] Li, Q., Yao, F. Z., Liu, Y., Zhang, G. Z., Wang, H., Wang, Q. (2018). High-temperature dielectric materials for electrical energy storage. *Annual Review of Materials Research*, 48: 219–243.

[11] Li, Q., Cheng, S. (2020). Polymer nanocomposites for high-energy-density capacitor dielectrics: Fundamentals and recent progress.

IEEE Electrical Insulation Magazine, 36: 7–28.

[12] Zhou, Y., Wang, Q. (2020). Advanced polymer dielectrics for high temperature capacitive energy storage. *Journal of Applied Physics*, 127: 240902.

[13] Li, H., Zhou, Y., Liu, Y., Li, L., Liu, Y., Wang, Q. (2021). Dielectric polymers for high-temperature capacitive energy storage. *Chemical Society Reviews*, 50: 6369–6400.

[14] Feng, M. J., Feng, Y., Zhang, T. D., Li, J. L., Chen, Q. G., Chi, Q. G., Lei, Q. Q. (2021). Recent advances in multilayer-structure dielectrics for energy storage application. *Advanced Science*, 8: 2102221.

[15] Michalczyk, P., Bramoulle, M. (2003). Ultimate properties of the polypropylene film for energy storage capacitors. *IEEE Transactions on Magnetics*, 39: 362–365.

[16] Rabuffi, M., Picci, G. (2002). Status quo and future prospects for metallized polypropylene energy storage capacitors. *IEEE Transactions on Plasma Science*, 30: 1939–1942.

[17] Li, W. J., Meng, Q. J., Zheng, Y. S., Zhang, Z. C., Xia, W. M., Xu, Z. (2010). Electric energy storage properties of poly(vinylidene fluoride). *Applied Physics Letters*, 96: 192905.

[18] Meng, N., Ren, X. T., Santagiuliana, G., Ventura, L., Zhang, H., Wu, J. Y., Yan, H. X., Reece, M. J., Bilotti, E. (2019). Ultrahigh β-phase content poly(vinylidene fluoride) with relaxor-like ferroelectricity for high energy density capacitors. *Nature Communications*, 10: 4535.

[19] Zhou, X., Chu, B. J., Neese, B., Lin, M. R., Zhang, Q. M. (2007). Electrical energy density and discharge characteristics of a poly(vinylidene fluoride-chlorotrifluoroethylene)copolymer. *IEEE Transactions on Dielectrics and Electrical Insulation*, 14: 1133–1138.

[20] Zhou, X., Zhao, X. H., Suo, Z. G., Zou, C., Runt, J., Liu, S., Zhang, S. H., Zhang, Q. M. (2009). Electrical breakdown and ultrahigh electrical energy density in poly(vinylidene fluoride-hexafluoropropylene) copolymer. *Applied Physics Letters*, 94: 162901.

[21] Gadinski, M. R., Han, K., Li, Q., Zhang, G. Z., Reainthippayasakul, W., Wang, Q. (2014). High energy density and breakdown strength from β and γ phases in poly(vinylidene fluoride-co-bromotrifluoroethylene) copolymers. *ACS Applied Materials & Interfaces*, 6: 18981–18988.

[22] Chu, B. J., Zhou, X., Neese, B., Zhang, Q. M., Bauer, F. (2006). Relaxor ferroelectric poly(vinylidene fluoride-trifluoroethylene-chlorofluoroethylene) terpolymer for high energy density storage capacitors. *IEEE Transactions on Dielectrics and Electrical Insulation*, 13: 1162–1169.

[23] Zhang, Z. C., Chung, T. C. M. (2007). Study of VDF/TrFE/CTFE terpolymers for high pulsed capacitor with high energy density and low energy loss. *Macromolecules*, 40: 783–785.

[24] Zhang, Z. C., Chung, T. C. M. (2007). The structure-property relationship of poly(vinylidene difluoride)-based polymers with energy storage and loss under applied electric fields. *Macromolecules*, 40: 9391–9397.

[25] Luo, B. C., Wang, X. H., Tian, E. K., Song, H. Z., Wang, H. X., Li, L. T. (2017). Enhanced energy-storage density and high efficiency of lead-free $CaTiO_3$-$BiScO_3$ linear dielectric ceramics. *ACS Applied Materials & Interfaces*, 9: 19963–19972.

[26] Love, G. R. (1990). Energy storage in ceramic dielectrics. *Journal of the American Ceramic Society*, 73: 323–328.

[27] Ogihara, H., Randall, C. A., Trolier-McKinstry, S. (2009). High-energy density capacitors utilizing $0.7BaTiO_3$-$0.3\ BiScO_3$ ceramics. *Journal of the American Ceramic Society*, 92: 1719–1724.

[28] Correia, T. M., McMillen, M., Rokosz, M. K., Weaver, P. M., Gregg, J. M., Viola, G., Cain, M. G. (2013). A lead-free and high-energy density ceramic for energy storage applications. *Journal of the American Ceramic Society*, 96: 2699–2702.

[29] Ahn, C. W., Amarsanaa, G., Won, S. S., Chae, S. A., Lee, D. S., Kim, I. W. (2015). Antiferroelectric thin-film capacitors with high energy-storage densities, low energy losses, and fast discharge times. *ACS Applied Materials & Interfaces*, 7: 26381–26386.

[30] Zhu, X. P., Shi, P., Lou, X. J., Gao, Y. F., Guo, X. D., Sun, H. N., Liu, Q. D., Ren, Z. J. (2020). Remarkably enhanced energy storage properties of lead-free $Ba_{0.53}Sr_{0.47}TiO_3$ thin films capacitors by optimizing bottom electrode thickness. *Journal of the European Ceramic Society*, 40: 5475–5482.

[31] Ieda, M. (1980). Dielectric breakdown process of polymers. *IEEE Transactions on Electrical Insulation*, EI-15: 206–224.

[32] Zebouchi, N., Bendaoud, M., Essolbi, R., Malec, D., Ai, B., Giam, H. T. (1996). Electrical breakdown theories applied to polyethylene terephthalate films under the combined effects of pressure and temperature. *Journal of Applied Physics*, 79: 2497–2501.

[33] Watson, J., Castro, G. (2015). A review of high-temperature electronics technology and applications. *Journal of Materials Science: Materials in Electronics*, 26: 9226–9235.

[34] Lovinger, A. J. (1983). Ferroelectric polymers. *Science* , 220: 1115–1121.

[35] Martins, P., Lopes, A. C., Lanceros-Mendez, S. (2014). Electroactive phases of poly(vinylidene fluoride): Determination, processing and applications. *Progress in Polymer Science*, 39: 683–706.

[36] Furukawa, T. (1989). Ferroelectric properties of vinylidene fluoride copolymers. *Phase Transitions*, 18: 143–211.

[37] Zhang, Q. M., Bharti, V. V., Zhao, X. (1998). Giant electrostriction and relaxor ferroelectric behavior in electron-irradiated poly(vinylidene fluoride-trifluoroethylene) copolymer. *Science*, 280: 2101–2104.

[38] Chu, B. J., Zhou, X., Ren, K. L., Neese, B., Lin, M. R., Wang, Q., Bauer, F., Zhang, Q. M. (2006). A dielectric polymer with high electric energy density and fast discharge speed. *Science* , 313: 334–336.

[39] Khanchaitit, P., Han, K., Gadinski, M. R., Li, Q., Wang, Q. (2013). Ferroelectric polymer networks with high energy density and improved discharged efficiency for dielectric energy storage. *Nature Communications*, 4: 2845.

[40] Chen, X. Z., Li, Z. W., Cheng, Z. X., Zhang, J. Z., Shen, Q. D., Ge, H. X., Li, H. T. (2011). Greatly enhanced energy density and patterned films induced by photo cross-linking of poly(vinylidene fluoride-chlorotrifluoroethylene). *Macromolecular Rapid Communications*, 32: 94–99.

[41] Guan, F. X., Pan, J. L., Wang, J., Wang, Q., Zhu, L. (2010). Crystal orientation effect on electric energy storage in poly(vinylidene fluoride-co-hexafluoropropylene) copolymers. *Macromolecules*, 43: 384–392.

[42] Hu, H. L., Zhang, F., Luo, S. B., Chang, W. K., Yue, J. L., Wang, C. H. (2020). Recent advances in rational design of polymer nanocomposite dielectrics for energy storage. *Nano Energy*, 74: 104844.

[43] Hu, J., Zhang, S. F., Tang, B. T. (2021). 2D filler-reinforced polymer nanocomposite dielectrics for high-k dielectric and energy storage applications. *Energy Storage Materials*, 34: 260–281.

[44] Bai, Y., Cheng, Z. Y., Bharti, V., Xu, H. S., Zhang, Q. M. (2000). High-dielectric-constant ceramic-powder polymer composites. *Applied Physics Letters*, 76: 3804–3806.

[45] Li, J. J., Claude, J., Norena-Franco, L. E., Seok, S. I., Wang, Q. (2008). Electrical energy storage in ferroelectric polymer nanocomposites containing surface-functionalized $BaTiO_3$ nanoparticles. *Chemistry of Materials*, 20: 6304–6306.

[46] Kim, P., Doss, N. M., Tillotson, J. P., Hotchkiss, P. J., Pan, M. J., Marder, S. R., Li, J. Y., Calame, J. P., Perry, J. W. (2009). High energy density nanocomposites based on surface-modified BaTiO(3) and a ferroelectric polymer. *ACS Nano*, 3: 2581–2592.

[47] Yu, K., Niu, Y. J., Zhou, Y. C., Bai, Y. Y., Wang, H. (2013). Nanocomposites of surface-modified $BaTiO_3$ nanoparticles filled ferroelectric polymer with enhanced energy density. *Journal of the American Ceramic Society*, 96: 2519–2524.

[48] Yu, K., Wang, H., Zhou, Y. C., Bai, Y. Y., Niu, Y. J. (2013). Enhanced dielectric properties of $BaTiO_3$/poly(vinylidene fluoride) nanocomposites for energy storage applications. *Journal of Applied Physics*, 113: 034105.

[49] Fu, J., Hou, Y. D., Zheng, M. P., Wei, Q. Y., Zhu, M. K., Yan, H.

(2015). Improving dielectric properties of PVDF composites by employing surface modified strong polarized $BaTiO_3$ particles derived by molten salt method. *ACS Applied Materials & Interfaces*, 7: 24480–24491.

[50] Luo, H., Zhang, D., Jiang, C., Yuan, X., Chen, C., Zhou, K. C. (2015). Improved dielectric properties and energy storage density of poly(vinylidene fluoride-co-hexafluoropropylene) nanocomposite with hydantoin epoxy resin coated $BaTiO_3$. *ACS Applied Materials & Interfaces*, 7: 8061–8069.

[51] Pan, Z. B., Yao, L. M., Zhai, J. W., Shen, B., Wang, H. T. (2017). Significantly improved dielectric properties and energy density of polymer nanocomposites via small loaded of $BaTiO_3$ nanotubes. *Composites Science and Technology*, 147: 30–38.

[52] Xie, Y. C., Yu, Y. Y., Feng, Y. F., Jiang, W. R., Zhang, Z. C. (2017). Fabrication of stretchable nanocomposites with high energy density and low loss from cross-linked PVDF filled with poly(dopamine) encapsulated $BaTiO_3$. *ACS Applied Materials & Interfaces*, 9: 2995–3005.

[53] Hu, P. H., Gao, S. M., Zhang, Y. Y., Zhang, L., Wang, C. C. (2018). Surface modified $BaTiO_3$ nanoparticles by titanate coupling agent induce significantly enhanced breakdown strength and larger energy density in PVDF nanocomposite. *Composites Science and Technology*, 156: 109–116.

[54] Niu, Y. J., Xiang, F., Wang, Y. F., Chen, J., Wang, H. (2018). Effect of the coverage level of carboxylic acids as a modifier for Barium titanate nanoparticles on the performance of poly(vinylidene fluoride)-based nanocomposites for energy storage applications. *Physical Chemistry Chemical Physics*, 20: 6598–6605.

[55] Ma, J. C., Zhang, Y. B., Zhang, Y., Zhang, L. Q., Zhang, S. X., Jiang, X. C., Liu, H. (2022). Constructing nanocomposites with robust covalent connection between nanoparticles and polymer for high discharged energy density and excellent tensile properties. *Journal of Energy Chemistry*, 68: 195–205.

[56] Song, Y., Shen, Y., Liu, H. Y., Lin, Y. H., Li, M., Nan, C. W. (2012). Enhanced dielectric and ferroelectric properties induced by dopamine-modified $BaTiO_3$ nanofibers in flexible poly(vinylidene fluoride-trifluoroethylene) nanocomposites. *Journal of Materials Chemistry*, 22: 8063–8068.

[57] Tang, H. X., Lin, Y. R., Sodano, H. A. (2013). Synthesis of high aspect ratio $BaTiO_3$ nanowires for high energy density nanocomposite capacitors. *Advanced Energy Materials*, 3: 451–456.

[58] Wang, G. Y., Huang, X. Y., Jiang, P. K. (2017). Bio-inspired fluoropolydopamine meets Barium titanate nanowires: a perfect combination to enhance energy storage capability of polymer nanocomposites. *ACS Applied Materials & Interfaces*, 9: 7547–7555.

[59] Xie, B., Zhang, H., Zhang, Q., Zang, J., Yang, C., Wang, Q., Li, M., Jiang, S. (2017). Enhanced energy density of polymer nanocomposites at a low electric field through aligned $BaTiO_3$ nanowires. *Journal of Materials Chemistry A*, 5: 6070–6078.

[60] Yao, L. M., Pan, Z. B., Zhai, J. W., Chen, H. H. D. (2017). Novel design of highly[110]-oriented Barium titanate nanorod array and its application in nanocomposite capacitors. *Nanoscale* , 9: 4255–4264.

[61] Song, Y., Shen, Y., Hu, P. H., Lin, Y. H., Li, M., Nan, C. W. (2012). Significant enhancement in energy density of polymer composites induced by dopamine-modified $Ba_{0.6}Sr_{0.4}TiO_3$ nanofibers. *Applied Physics Letters*, 101: 152904.

[62] Xia, W. M., Xu, Z., Wen, F., Zhang, Z. C. (2012). Electrical energy density and dielectric properties of poly(vinylidene fluoride-chlorotrifluoroethylene)/$BaSrTiO_3$ nanocomposites. *Ceramics International*, 38: 1071–1075.

[63] Tang, H. X., Sodano, H. A. (2013). Ultra high energy density nanocomposite capacitors with fast discharge using $Ba_{0.2}Sr_{0.8}TiO_3$ nanowires. *Nano Letters*, 13: 1373–1379.

[64] Liu, S., Zhai, J. (2014). A small loading of surface-modified $Ba_{0.6}Sr_{0.4}TiO_3$ nanofiber-filled nanocomposites with enhanced dielectric constant and energy density. *RSC Advances*, 4: 40973–40979.

[65] Liu, S. H., Zhai, J. W., Wang, J. W., Xue, S. X., Zhang, W. Q. (2014). Enhanced energy storage density in poly(vinylidene fluoride) nanocomposites by a small loading of suface-hydroxylated $Ba_{0.6}Sr_{0.4}TiO_3$ nanofibers. *ACS Applied Materials & Interfaces*, 6: 1533–1540.

[66] Shen, Y., Hu, Y. H., Chen, W. W., Wang, J. J., Guan, Y. H., Du, J. W., Zhang, X., Ma, J., Li, M., Lin, Y. H., et al. (2015). Modulation of topological structure induces ultrahigh energy density of graphene/$Ba_{0.6}Sr_{0.4}TiO_3$ nanofiber/polymer nanocomposites. *Nano Energy*, 18: 176–186.

[67] Tang, H. X., Lin, Y. R., Sodano, H. A. (2012). Enhanced energy storage in nanocomposite capacitors through aligned PZT nanowires by uniaxial strain assembly. *Advanced Energy Materials*, 2: 469–476.

[68] Zhang, D., Liu, W. W., Guo, R., Zhou, K. C., Luo, H. (2018). High discharge energy density at low electric field using an aligned titanium dioxide/lead zirconate titanate nanowire array. *Advanced Science*, 5: 1700512.

[69] Liu, S. H., Zhai, J. W. (2015). Improving the dielectric constant and energy density of poly(vinylidene fluoride) composites induced by surface-modified $SrTiO_3$ nanofibers by polyvinylpyrrolidone. *Journal of Materials Chemistry A*, 3: 1511–1517.

[70] Yao, L. M., Pan, Z. B., Zhai, J. W., Zhang, G. Z., Liu, Z. Y., Liu, Y. H. (2018). High-energy-density with polymer nanocomposites containing of $SrTiO_3$ nanofibers for capacitor application. *Composites Part A: Applied Science and Manufacturing*, 109: 48–54.

[71] Liu, S. H., Xue, S. X., Xiu, S. M., Shen, B., Zhai, J. W. (2016). Surface-modified $Ba(Zr_{0.3}Ti_{0.7})O_3$ nanofibers by polyvinylpyrrolidone filler for poly(vinylidene fluoride) composites with enhanced dielectric constant and energy storage density. *Scientific Reports*, 6: 26198.

[72] Luo, H., Roscow, J., Zhou, X. F., Chen, S., Han, X. H., Zhou, K. C., Zhang, D., Bowen, C. R. (2017). Ultra-high discharged energy density capacitor using high aspect ratio $Na_{0.5}Bi_{0.5}TiO_3$ nanofibers. *Journal of Materials Chemistry A*, 5: 7091–7102.

[73] Pan, Z. B., Yao, L. M., Zhai, J. W., Wang, H. T., Shen, B. (2017). Ultrafast discharge and enhanced energy density of polymer nanocomposites loaded with $0.5(Ba_{0.7}Ca_{0.3})TiO_3$-$0.5Ba(Zr_{0.2}Ti_{0.8})O_3$ one-dimensional nanofibers. *ACS Applied Materials & Interfaces*, 9: 14337–14346.

[74] Li, J. J., Seok, S. I., Chu, B. J., Dogan, F., Zhang, Q. M., Wang, Q. (2009). Nanocomposites of ferroelectric polymers with TiO_2 nanoparticles exhibiting significantly enhanced electrical energy density. *Advanced Materials*, 21: 217–221.

[75] Li, J. J., Khanchaitit, P., Han, K., Wang, Q. (2010). New route toward high-energy-density nanocomposites based on chain-end functionalized ferroelectric polymers. *Chemistry of Materials*, 22: 5350–5357.

[76] Tang, H. X., Sodano, H. A. (2013). High energy density nanocomposite capacitors using non-ferroelectric nanowires. *Applied Physics Letters*, 102: 063901.

[77] Chen, S. S., Hu, J., Gao, L., Zhou, Y., Peng, S. M., He, J. L., Dang, Z. M. (2016). Enhanced breakdown strength and energy density in PVDF nanocomposites with functionalized MgO nanoparticles. *RSC Advances*, 6: 33599–33605.

[78] Yao, L. M., Pan, Z. B., Liu, S. H., Zhai, J. W., Chen, H. H. D. (2016). Significantly enhanced energy density in nanocomposite capacitors combining the TiO_2 nanorod array with poly(vinylidene fluoride). *ACS Applied Materials & Interfaces*, 8: 26343–26351.

[79] Li, L., Feng, R., Zhang, Y., Dong, L. J. (2017). Flexible, transparent and high dielectric-constant fluoropolymer-based nanocomposites with a fluoride-constructed interfacial structure. *Journal of Materials Chemistry C*, 5: 11403–11410.

[80] Wang, G. Y., Huang, X. Y., Jiang, P. K. (2017). Bio-inspired polydopamine coating as a facile approach to constructing polymer nanocomposites for energy storage. *Journal of Materials Chemistry C*, 5: 3112–3120.

[81] Li, H., Yang, T. N., Zhou, Y., Ai, D., Yao, B., Liu, Y., Li, L.,

Chen, L. Q., Wang, Q. (2021). Enabling high-energy-density high-efficiency ferroelectric polymer nanocomposites with rationally designed nanofillers. *Advanced Functional Materials*, 31: 2006739.

[82] Zhang, Q. L., Zhang, Z., Xu, N. X., Yang, H. (2020). Dielectric properties of P(VDF-TrFE-CTFE) composites filled with surface-coated TiO_2 nanowires by SnO_2 nanoparticles. *Polymers*, 12: 85.

[83] Li, Q., Han, K., Gadinski, M. R., Zhang, G. Z., Wang, Q. (2014). High energy and power density capacitors from solution-processed ternary ferroelectric polymer nanocomposites. *Advanced Materials*, 26: 6244–6249.

[84] Li, Q., Zhang, G. Z., Liu, F. H., Han, K., Gadinski, M. R., Xiong, C. X., Wang, Q. (2015). Solution-processed ferroelectric terpolymer nanocomposites with high breakdown strength and energy density utilizing boron nitride nanosheets. *Energy & Environmental Science*, 8: 922–931.

[85] Jiang, J. Y., Shen, Z. H., Cai, X. K., Qian, J. F., Dan, Z. K., Lin, Y. H., Liu, B. L., Nan, C. W., Chen, L. Q., Shen, Y. (2019). Polymer nanocomposites with interpenetrating gradient structure exhibiting ultrahigh discharge efficiency and energy density. *Advanced Energy Materials*, 9: 1803411.

[86] Zhu, Y. K., Zhu, Y. J., Huang, X. Y., Chen, J., Li, Q., He, J. L., Jiang, P. K. (2019). High energy density polymer dielectrics interlayered by assembled boron nitride nanosheets. *Advanced Energy Materials*, 9: 1901826.

[87] Li, Y. X., Wang, Z., Kong, M. L., Yi, Z. H. (2021). Improved thermal conductivity and breakdown strength of PVDF-based composites by improving the dispersion of BN. *High Voltage*.

[88] Liu, Y. H., Wen, Y. Y., Xu, W. W., Li, B., Song, Z. M., Li, Y. Y., Xia, F. (2021). Improving the energy density of P(VDF-HFP)/boron nitride nanosheets nanocomposites by using the third phase filler with high dielectric constant. *Journal of Polymer Research*, 28: 411.

[89] Shang, Y. N., Feng, Y., Li, C. M., Zhang, C. H., Zhang, T. D., Zhang, Y. Q., Zhang, Y., Song, C. H., Chi, Q. G. (2022). Energy storage properties of P(VDF-TrFE-CTFE)-based composite dielectrics with uniform and gradient-doped boron nitride nanosheets. *IET Nanodielectrics*, 5: 50–61.

[90] Han, K., Li, Q., Chen, Z. Y., Gadinski, M. R., Dong, L. J., Xiong, C. X., Wang, Q. (2013). Suppression of energy dissipation and enhancement of breakdown strength in ferroelectric polymer-graphene percolative composites. *Journal of Materials Chemistry C*, 1: 7034–7042.

[91] Jia, Q. C., Huang, X. Y., Wang, G. Y., Diao, J. C., Jiang, P. K. (2016). MoS_2 nanosheet superstructures based polymer composites for high-dielectric and electrical energy storage applications. *The Journal of Physical Chemistry C*, 120: 10206–10214.

[92] Zhang, X., Shen, Y., Zhang, Q. H., Gu, L., Hu, Y. H., Du, J. W., Lin, Y. H., Nan, C. W. (2015). Ultrahigh energy density of polymer nanocomposites containing $BaTiO_3$@TiO_2 nanofibers by atomic-scale interface engineering. *Advanced Materials*, 27: 819–824.

[93] Zhang, X., Shen, Y., Xu, B., Zhang, Q. H., Gu, L., Jiang, J. Y., Ma, J., Lin, Y. H., Nan, C. W. (2016). Giant energy density and improved discharge efficiency of solution-processed polymer nanocomposites for dielectric energy storage. *Advanced Materials*, 28: 2055–2061.

[94] Pan, Z. B., Yao, L. M., Zhai, J. W., Fu, D. Z., Shen, B., Wang, H. T. (2017). High-energy-density polymer nanocomposites composed of newly structured one-dimensional $BaTiO_3$@Al_2O_3 nanofibers. *ACS Applied Materials & Interfaces*, 9: 4024–4033.

[95] Jiang, Y. C., Wang, J. B., Zhang, Q. L., Yang, H., Shen, D., Zhou, F. M. (2019). Enhanced dielectric performance of P(VDF-HFP) composites filled with Ni@polydopamine@$BaTiO_3$ nanowires. *Colloids and Surfaces A: Physicochemical and Engineering Aspects*, 576: 55–62.

[96] Jiang, Y. C., Zhang, Z., Zhou, Z., Yang, H., Zhang, Q. L. (2019). Enhanced dielectric performance of P(VDF-HFP) composites with satellite-core-structured Fe_2O_3@$BaTiO_3$ nanofillers. *Polymers*, 11: 1541.

[97] Luo, S. B., Yu, J. Y., Yu, S. H., Sun, R., Cao, L. Q., Liao, W. H., Wong, C. P. (2019). Significantly enhanced electrostatic energy storage performance of flexible polymer composites by introducing highly insulating-ferroelectric microhybrids as fillers. *Advanced Energy Materials*, 9: 1803204.

[98] Li, Y. S., Zhou, Y., Zhu, Y. J., Cheng, S., Yuan, C., Hu, J., He, J. L., Li, Q. (2020). Polymer nanocomposites with high energy density and improved charge-discharge efficiency utilizing hierarchically-structured nanofillers. *Journal of Materials Chemistry A*, 8: 6576–6585.

[99] Wang, P. J., Zhou, D., Li, J., Pang, L. X., Liu, W. F., Su, J. Z., Singh, C., Trukhanov, S., Trukhanov, A. (2020). Significantly enhanced electrostatic energy storage performance of P(VDF-HFP)/$BaTiO_3$-Bi($Li_{0.5}Nb_{0.5}$)O_3 nanocomposites. *Nano Energy*, 78: 105247.

[100] Xiong, X. Y., Zhang, Q. L., Zhang, Z., Yang, H., Tong, J. X., Wen, J. Y. (2021). Superior energy storage performance of PVDF-based composites induced by a novel nanotube structural BST@SiO_2 filler. *Composites Part A: Applied Science and Manufacturing*, 145: 106375.

[101] Huang, X. Y., Jiang, P. K. (2015). Core-shell structured high-k polymer nanocomposites for energy storage and dielectric applications. *Advanced Materials*, 27: 546–554.

[102] Yang, K., Huang, X. Y., Huang, Y. H., Xie, L. Y., Jiang, P. K. (2013). Fluoro-Polymer@$BaTiO_3$ hybrid nanoparticles prepared via RAFT polymerization: toward ferroelectric polymer nanocomposites with high dielectric constant and low dielectric loss for energy storage application. *Chemistry of Materials*, 25: 2327–2338.

[103] Zhu, M., Huang, X. Y., Yang, K., Zhai, X., Zhang, J., He, J. L., Jiang, P. K. (2014). Energy storage in ferroelectric polymer nanocomposites filled with core-shell structured polymer@$BaTiO_3$ nanoparticles: Understanding the role of polymer shells in the interfacial regions. *ACS Applied Materials & Interfaces*, 6: 19644–19654.

[104] Rahimabady, M., Mirshekarloo, M. S., Yao, K., Lu, L. (2013). Dielectric behaviors and high energy storage density of nanocomposites with core-shell $BaTiO_3$@TiO_2 in poly(vinylidene fluoride-hexafluoropropylene). *Physical Chemistry Chemical Physics*, 15: 16242–16248.

[105] Yu, K., Niu, Y. J., Bai, Y. Y., Zhou, Y. C., Wang, H. (2013). Poly(vinylidene fluoride) polymer based nanocomposites with significantly reduced energy loss by filling with core-shell structured $BaTiO_3$/SiO_2 nanoparticles. *Applied Physics Letters*, 102: 102903.

[106] Liu, S. H., Xue, S. X., Shen, B., Zhai, J. W. (2015). Reduced energy loss in poly(vinylidene fluoride) nanocomposites by filling with a small loading of core-shell structured $BaTiO_3$/SiO_2 nanofibers. *Applied Physics Letters*, 107: 032907.

[107] Pan, Z. B., Yao, L. M., Zhai, J. W., Shen, B., Liu, S. H., Wang, H. T., Liu, J. H. (2016). Excellent energy density of polymer nanocomposites containing $BaTiO_3$@Al_2O_3 nanofibers induced by moderate interfacial area. *Journal of Materials Chemistry A*, 4: 13259–13264.

[108] Prateek, Bhunia, R., Siddiqui, S., Garg, A., Gupta, R. K. (2019). Significantly enhanced energy density by tailoring the interface in hierarchically structured TiO_2-$BaTiO_3$-TiO_2 nanofillers in PVDF-based thin-film polymer nanocomposites. *ACS Applied Materials & Interfaces*, 11: 14329–14339.

[109] Wang, P. J., Zhou, D., Guo, H. H., Liu, W. F., Su, J. Z., Fu, M. S., Singh, C., Trukhanov, S., Trukhanov, A. (2020). Ultrahigh enhancement rate of the energy density of flexible polymer nanocomposites using core-shell $BaTiO_3$@MgO structures as the filler. *Journal of Materials Chemistry A*, 8: 11124–11132.

[110] Chen, J., Zhang, X. Y., Yang, X., Li, C. Y., Wang, Y. F., Chen, W. X. (2021). High breakdown strength and energy storage density in aligned $SrTiO_3$@SiO_2 core-shell platelets incorporated polymer composites. *Membranes*, 11: 756.

[111] Pan, Z. B., Zhai, J. W., Shen, B. (2017). Multilayer hierarchical interfaces with high energy density in polymer nanocomposites composed of $BaTiO_3$@TiO_2@Al_2O_3 nanofibers. *Journal of Materials*

Chemistry A, 5: 15217–15226.

[112] Jiang, J. Y., Shen, Z. H., Qian, J. F., Dan, Z. K., Guo, M. F., He, Y., Lin, Y. H., Nan, C. W., Chen, L. Q., Shen, Y. (2019). Synergy of micro-/mesoscopic interfaces in multilayered polymer nanocomposites induces ultrahigh energy density for capacitive energy storage. *Nano Energy*, 62: 220–229.

[113] Zhou, X., Chen, Q., Zhang, Q. M., Zhang, S. H. (2011). Dielectric behavior of bilayer films of P(VDF-CTFE) and low temperature PECVD fabricated Si_3N_4. *IEEE Transactions on Dielectrics and Electrical Insulation*, 18: 463–470.

[114] Chen, C., Xing, J. W., Cui, Y., Zhang, C. H., Feng, Y., Zhang, Y. Q., Zhang, T. D., Chi, Q. G., Wang, X., Lei, Q. Q. (2020). Designing of ferroelectric/linear dielectric bilayer films: An effective way to improve the energy storage performances of polymer-based capacitors. *The Journal of Physical Chemistry C*, 124: 5920–5927.

[115] Pei, J. Y., Zhong, S. L., Zhao, Y., Yin, L. J., Feng, Q. K., Huang, L., Liu, D. F., Zhang, Y. X., Dang, Z. M. (2021). All-organic dielectric polymer films exhibiting superior electric breakdown strength and discharged energy density by adjusting the electrode-dielectric interface with an organic nano-interlayer. *Energy & Environmental Science*, 14: 5513–5522.

[116] Wang, Y. F., Cui, J., Yuan, Q. B., Niu, Y. J., Bai, Y. Y., Wang, H. (2015). Significantly enhanced breakdown strength and energy density in sandwich-structured Barium titanate/poly(vinylidene fluoride) nanocomposites. *Advanced Materials*, 27: 6658–6663.

[117] Wang, Y. F., Wang, L. X., Yuan, Q. B., Niu, Y. J., Chen, J., Wang, Q., Wang, H. (2017). Ultrahigh electric displacement and energy density in gradient layer-structured $BaTiO_3$/PVDF nanocomposites with an interfacial barrier effect. *Journal of Materials Chemistry A*, 5: 10849–10855.

[118] Jiang, Y. D., Zhang, X., Shen, Z. H., Li, X. H., Yan, J. J., Li, B. W., Nan, C. W. (2020). Ultrahigh breakdown strength and improved energy density of polymer nanocomposites with gradient distribution of ceramic nanoparticles. *Advanced Functional Materials*, 30: 1906112.

[119] Zhang, X., Jiang, J. Y., Shen, Z. H., Dan, Z. K., Li, M., Lin, Y. H., Nan, C. W., Chen, L. Q., Shen, Y. (2018). Polymer nanocomposites with ultrahigh energy density and high discharge efficiency by modulating their nanostructures in three dimensions. *Advanced Materials*, 30: 1707269.

[120] Liu, F. H., Li, Q., Cui, J., Li, Z. Y., Yang, G., Liu, Y., Dong, L. J., Xiong, C. X., Wang, H., Wang, Q. (2017). High-energy-density dielectric polymer nanocomposites with trilayered architecture. *Advanced Functional Materials*, 27: 1606292.

[121] Cui, Y., Zhang, T. D., Feng, Y., Zhang, C. H., Chi, Q. G., Zhang, Y. Q., Chen, Q. G., Wang, X., Lei, Q. Q. (2019). Excellent energy storage density and efficiency in blend polymer-based composites by design of core-shell structured inorganic fibers and sandwich structured films. *Composites Part B: Engineering*, 177: 107429.

[122] Lin, Y., Sun, C., Zhan, S. L., Zhang, Y. J., Yuan, Q. B. (2020). Ultrahigh discharge efficiency and high energy density in sandwich structure $K_{0.5}Na_{0.5}NbO_3$ nanofibers/poly(vinylidene fluoride) composites. *Advanced Materials Interfaces*, 7: 2000033.

[123] Lin, Y., Zhang, Y. J., Zhan, S. L., Sun, C., Hu, G. L., Yang, H. B., Yuan, Q. B. (2020). Synergistically ultrahigh energy storage density and efficiency in designed sandwich-structured poly(vinylidene fluoride)-based flexible composite films induced by doping $Na_{0.5}Bi_{0.5}TiO_3$ whiskers. *Journal of Materials Chemistry A*, 8: 23427–23435.

[124] Marwat, M. A., Yasar, M., Ma, W. G., Fan, P. Y., Liu, K., Lu, D. J., Tian, Y., Samart, C., Ye, B. H., Zhang, H. B. (2020). Significant energy density of discharge and charge-discharge efficiency in Ag@BNN nanofillers-modified heterogeneous sandwich structure nanocomposites. *ACS Applied Energy Materials*, 3: 6591–6601.

[125] Li, Z. Y., Shen, Z. H., Yang, X., Zhu, X. M., Zhou, Y., Dong, L. J., Xiong, C. X., Wang, Q. (2021). Ultrahigh charge-discharge efficiency and enhanced energy density of the sandwiched polymer nanocomposites with poly(methyl methacrylate) layer. *Composites Science and Technology*, 202: 108591.

[126] Sun, S. B., Shi, Z. C., Liang, L., Li, T., Zhang, S. L., Xu, W. F., Han, M. L., Zhang, M. Y. (2021). Simultaneous realization of significantly enhanced breakdown strength and moderately enhanced permittivity in layered PMMA/P(VDF-HFP) nanocomposites via inserting an Al_2O_3/P(VDF-HFP) layer. *The Journal of Physical Chemistry C*, 125: 22379–22387.

[127] Xie, H. R., Wang, L., Gao, X., Luo, H., Liu, L. H., Zhang, D. (2020). High breakdown strength and energy density in multilayer-structured ferroelectric composite. *ACS Omega*, 5: 32660–32666.

[128] Li, L., Cheng, J. S., Cheng, Y. Y., Han, T., Liang, X., Zhao, Y., Zhao, G. H., Dong, L. J. (2020). Polymer dielectrics exhibiting an anomalously improved dielectric constant simultaneously achieved high energy density and efficiency enabled by CdSe/$Cd_{1-x}Zn_xS$ quantum dots. *Journal of Materials Chemistry A*, 8: 13659–13670.

[129] Li, L., Cheng, J. S., Cheng, Y. Y., Han, T., Liu, Y., Zhou, Y., Zhao, G. H., Zhao, Y., Xiong, C. X., Dong, L. J., et al. (2021). Significant improvements in dielectric constant and energy density of ferroelectric polymer nanocomposites enabled by ultralow contents of nanofillers. *Advanced Materials*, 33: 2102392.

[130] Rahimabady, M., Chen, S. T., Yao, K., Eng Hock Tay, F., Lu, L. (2011). High electric breakdown strength and energy density in vinylidene fluoride oligomer/poly(vinylidene fluoride) blend thin films. *Applied Physics Letters*, 99: 142901.

[131] Zhang, C. H., Zhang, T. Q., Feng, M. J., Cui, Y., Zhang, T. D., Zhang, Y. Q., Feng, Y., Zhang, Y., Chi, Q. G., Liu, X. L. (2021). Significantly improved energy storage performance of PVDF ferroelectric films by blending PMMA and filling PCBM. *ACS Sustainable Chemistry & Engineering*, 9: 16291–16303.

[132] Ma, R., Baldwin, A. F., Wang, C. C., Offenbach, I., Cakmak, M., Ramprasad, R., Sotzing, G. A. (2014). Rationally designed polyimides for high-energy density capacitor applications. *ACS Applied Materials & Interfaces*, 6: 10445–10451.

[133] Wei, J. J., Zhang, Z. B., Tseng, J. K., Treufeld, I., Liu, X. B., Litt, M. H., Zhu, L. (2015). Achieving high dielectric constant and low loss property in a dipolar glass polymer containing strongly dipolar and small-sized sulfone groups. *ACS Applied Materials & Interfaces*, 7: 5248–5257.

[134] Zhang, Z. B., Wang, D. H., Litt, M. H., Tan, L. S., Zhu, L. (2018). High-temperature and high-energy-density dipolar glass polymers based on sulfonylated poly(2,6-dimethyl-1,4-phenylene oxide). *Angewandte Chemie International Edition*, 57: 1528–1531.

[135] Li, Z. Z., Treich, G. M., Tefferi, M., Wu, C., Nasreen, S., Scheirey, S. K., Ramprasad, R., Sotzing, G., Cao, Y. (2019). High energy density and high efficiency all-organic polymers with enhanced dipolar polarization. *Journal of Materials Chemistry A*, 7: 15026–15030.

[136] Zhang, Z. B., Zheng, J. F., Premasiri, K., Kwok, M. H., Li, Q., Li, R. P., Zhang, S. B., Litt, M. H., Gao, X. P. A., Zhu, L. (2020). High-κ polymers of intrinsic microporosity: A new class of high temperature and low loss dielectrics for printed electronics. *Materials Horizons*, 7: 592–597.

[137] Feng, Y., Jiang, L. H., Yang, A. Q., Liu, X., Yang, L. Q., Lu, G. H., Li, S. T. (2022). Interfacial effect on dielectric properties of self-assembled polythiourea-based copolymers for ultrahigh energy storage. *Macromolecular Rapid Communications*, 43: 2100700.

[138] Wu, Z. Q., Guo, Q., Liu, Y., Zhou, H. H., Zheng, H., Lei, X. F., Gong, L., Chen, Y. H., Liu, Z. G., Zhang, Q. Y. (2021). Excellent polyimide dielectrics containing conjugated ACAT for high-temperature polymer film capacitor. *Macromolecular Materials and Engineering*, 306: 2100456.

[139] Li, H., Yao, B., Zhou, Y., Xu, W. H., Ren, L. L., Ai, D., Wang, Q. (2020). Bilayer-structured polymer nanocomposites exhibiting high breakdown strength and energy density via interfacial barrier design. *ACS Applied Energy Materials*, 3: 8055–8063.

[140] Jiang, J. H., Li, J. P., Qian, J., Liu, X. Y., Zuo, P. Y., Yuan, Y., Zhuang, Q. X. (2021). Benzoxazole-polymer@CCTO hybrid nanoparticles prepared via RAFT polymerization: toward poly(p-

phenylene benzobisoxazole) nanocomposites with enhanced high-temperature dielectric properties. *Journal of Materials Chemistry A*, 9: 26010–26018.

[141] Li, L., Cheng, J. S., Cheng, Y. Y., Han, T., Liu, Y., Zhou, Y., Han, Z. B., Zhao, G. H., Zhao, Y., Xiong, C. X., et al. (2021). Significantly enhancing the dielectric constant and breakdown strength of linear dielectric polymers by utilizing ultralow loadings of nanofillers. *Journal of Materials Chemistry A*, 9: 23028–23036.

[142] Li, Y. P., Yin, J. H., Feng, Y., Li, J. L., Zhao, H., Zhu, C. C., Yue, D., Liu, Y. P., Su, B., Liu, X. X. (2022). Metal-organic Framework/Polyimide composite with enhanced breakdown strength for flexible capacitor. *Chemical Engineering Journal*, 429: 132228.

[143] Pan, J. L., Li, K., Li, J. J., Hsu, T., Wang, Q. (2009). Dielectric characteristics of poly(ether ketone ketone) for high temperature capacitive energy storage. *Applied Physics Letters*, 95: 022902.

[144] Tan, D., Zhang, L. L., Chen, Q., Irwin, P. (2014). High-temperature capacitor polymer films. *Journal of Electronic Materials*, 43: 4569–4575.

[145] Cheng, Z. X., Lin, M. R., Wu, S., Thakur, Y., Zhou, Y., Jeong, D. Y., Shen, Q. D., Zhang, Q. M. (2015). Aromatic poly(arylene ether urea) with high dipole moment for high thermal stability and high energy density capacitors. *Applied Physics Letters*, 106: 202902.

[146] Ho, J. S., Greenbaum, S. G. (2018). Polymer capacitor dielectrics for high temperature applications. *ACS Applied Materials & Interfaces*, 10: 29189–29218.

[147] Pan, J. L., Li, K., Chuayprakong, S., Hsu, T., Wang, Q. (2010). High-temperature poly(phthalazinone ether ketone) thin films for dielectric energy storage. *ACS Applied Materials & Interfaces*, 2: 1286–1289.

[148] Wu, C., Deshmukh, A. A., Li, Z. Z., Chen, L. H., Alamri, A., Wang, Y. F., Ramprasad, R., Sotzing, G. A., Cao, Y. (2020). Flexible temperature-invariant polymer dielectrics with large bandgap. *Advanced Materials*, 32: 2000499.

[149] Tang, Y. D., Xu, W. H., Niu, S., Zhang, Z. C., Zhang, Y. H., Jiang, Z. H. (2021). Crosslinked dielectric materials for high-temperature capacitive energy storage. *Journal of Materials Chemistry A*, 9: 10000–10011.

[150] Li, H., Gadinski, M. R., Huang, Y. Q., Ren, L. L., Zhou, Y., Ai, D., Han, Z. B., Yao, B., Wang, Q. (2020). Crosslinked fluoropolymers exhibiting superior high-temperature energy density and charge-discharge efficiency. *Energy & Environmental Science*, 13: 1279–1286.

[151] Sun, W. D., Lu, X. J., Jiang, J. Y., Zhang, X., Hu, P. H., Li, M., Lin, Y. H., Nan, C. W., Shen, Y. (2017). Dielectric and energy storage performances of polyimide/$BaTiO_3$ nanocomposites at elevated temperatures. *Journal of Applied Physics*, 121: 244101.

[152] Xu, W. H., Yang, G., Jin, L., Liu, J., Zhang, Y. H., Zhang, Z. C., Jiang, Z. H. (2018). High-k polymer nanocomposites filled with hyperbranched phthalocyanine-coated $BaTiO_3$ for high-temperature and elevated field applications. *ACS Applied Materials & Interfaces*, 10: 11233–11241.

[153] Jian, G., Jiao, Y., Meng, Q. Z., Xue, F., Feng, L., Yang, N., Jiang, J. H., Lü, M. F. (2021). Polyimide composites containing confined tetragonality high TC $PbTiO_3$ nanofibers for high-temperature energy storage. *Composites Part B: Engineering*, 224: 109190.

[154] Miao, W. J., Chen, H. X., Pan, Z. B., Pei, X. L., Li, L., Li, P., Liu, J. J., Zhai, J. W., Pan, H. (2021). Enhancement thermal stability of polyetherimide-based nanocomposites for applications in energy storage. *Composites Science and Technology*, 201: 108501.

[155] Liu, J., Shen, Z. H., Xu, W. H., Zhang, Y., Qian, X. S., Jiang, Z. H., Zhang, Y. H. (2020). Interface-strengthened polymer nanocomposites with reduced dielectric relaxation exhibit high energy density at elevated temperatures utilizing a facile dual crosslinked network. *Small*, 16: 2000714.

[156] Li, Q., Chen, L., Gadinski, M. R., Zhang, S., Zhang, G., Li, H. U., Iagodkine, E., Haque, A., Chen, L. Q., Jackson, T. N., et al. (2015). Flexible high-temperature dielectric materials from polymer nanocomposites. *Nature*, 523: 576–579.

[157] Zhang, K. Y., Ma, Z. Y., Deng, H., Fu, Q. (2022). Improving high-temperature energy storage performance of PI dielectric capacitor films through boron nitride interlayer. *Advanced Composites and Hybrid Materials*, 5: 238–249.

[158] Xu, W. H., Liu, J., Chen, T. W., Jiang, X. Y., Qian, X. S., Zhang, Y., Jiang, Z. H., Zhang, Y. H. (2019). Bioinspired polymer nanocomposites exhibit giant energy density and high efficiency at high temperature. *Small*, 15: 1901582.

[159] Li, H., Ai, D., Ren, L. L., Yao, B., Han, Z. B., Shen, Z. H., Wang, J. J., Chen, L. Q., Wang, Q. (2019). Scalable polymer nanocomposites with record high-temperature capacitive performance enabled by rationally designed nanostructured inorganic fillers. *Advanced Materials*, 31: 1900875.

[160] Klein, R. J., Barber, P., Chance, W. M., zur Loye, H. C. (2012). Covalently modified organic nanoplatelets and their use in polymer film capacitors with high dielectric breakdown and wide temperature operation. *IEEE Transactions on Dielectrics and Electrical Insulation*, 19: 1234–1238.

[161] Ai, D., Li, H., Zhou, Y., Ren, L. L., Han, Z. B., Yao, B., Zhou, W., Zhao, L., Xu, J. M., Wang, Q. (2020). Tuning nanofillers in *in situ* prepared polyimide nanocomposites for high-temperature capacitive energy storage. *Advanced Energy Materials*, 10: 1903881.

[162] Ren, L. L., Yang, L. J., Zhang, S. Y., Li, H., Zhou, Y., Ai, D., Xie, Z. L., Zhao, X. T., Peng, Z. R., Liao, R. J., et al. (2021). Largely enhanced dielectric properties of polymer composites with HfO_2 nanoparticles for high-temperature film capacitors. *Composites Science and Technology*, 201: 108528.

[163] Ren, L. L., Li, H., Xie, Z. L., Ai, D., Zhou, Y., Liu, Y., Zhang, S. Y., Yang, L. J., Zhao, X. T., Peng, Z. R., et al. (2021). High-temperature high-energy-density dielectric polymer nanocomposites utilizing inorganic core-shell nanostructured nanofillers. *Advanced Energy Materials*, 11: 2101297.

[164] Li, H., Ren, L. L., Ai, D., Han, Z. B., Liu, Y., Yao, B., Wang, Q. (2020). Ternary polymer nanocomposites with concurrently enhanced dielectric constant and breakdown strength for high-temperature electrostatic capacitors. *InfoMat*, 2: 389–400.

[165] Azizi, A., Gadinski, M. R., Li, Q., AlSaud, M. A., Wang, J. J., Wang, Y., Wang, B., Liu, F. H., Chen, L. Q., Alem, N., et al. (2017). High-performance polymers sandwiched with chemical vapor deposited hexagonal boron nitrides as scalable high-temperature dielectric materials. *Advanced Materials*, 29: 1701864.

[166] Zhou, Y., Li, Q., Dang, B., Yang, Y., Shao, T., Li, H., Hu, J., Zeng, R., He, J. L., Wang, Q. (2018). A scalable, high-throughput, and environmentally benign approach to polymer dielectrics exhibiting significantly improved capacitive performance at high temperatures. *Advanced Materials*, 30: 1805672.

[167] Zhang, T. D., Yang, L. Y., Ruan, J. Y., Zhang, C. H., Chi, Q. G. (2021). Improved high-temperature energy storage performance of PEI dielectric films by introducing an SiO_2 insulating layer. *Macromolecular Materials and Engineering*, 306: 2100514.

[168] Cheng, S., Zhou, Y., Hu, J., He, J. L., Li, Q. (2020). Polyimide films coated by magnetron sputtered boron nitride for high-temperature capacitor dielectrics. *IEEE Transactions on Dielectrics and Electrical Insulation*, 27: 498–503.

[169] Cheng, S., Zhou, Y., Li, Y. S., Yuan, C., Yang, M. C., Fu, J., Hu, J., He, J. L., Li, Q. (2021). Polymer dielectrics sandwiched by medium-dielectric-constant nanoscale deposition layers for high-temperature capacitive energy storage. *Energy Storage Materials*, 42: 445–453.

[170] Liu, G., Zhang, T. D., Feng, Y., Zhang, Y. Q., Zhang, C. H., Zhang, Y., Wang, X. B., Chi, Q. G., Chen, Q. G., Lei, Q. Q. (2020). Sandwich-structured polymers with electrospun boron nitrides layers as high-temperature energy storage dielectrics. *Chemical Engineering Journal*, 389: 124443.

[171] Dong, J., Hu, R., Xu, X., Chen, J., Niu, Y., Wang, F., Hao, J., Wu, K., Wang, Q., Wang, H. (2021). A facile in situ surface-functionalization approach to scalable laminated high-temperature polymer

dielectrics with ultrahigh capacitive performance. *Advanced Functional Materials*, 31: 2102644.

[172] Li, Q., Liu, F. H., Yang, T. N., Gadinski, M. R., Zhang, G. Z., Chen, L. Q., Wang, Q. (2016). Sandwich-structured polymer nanocomposites with high energy density and great charge-discharge efficiency at elevated temperatures. *Proceedings of the National Academy of Sciences of the United States of America*, 113: 9995–10000.

[173] Wang, P., Yao, L. M., Pan, Z. B., Shi, S. H., Yu, J. H., Zhou, Y., Liu, Y., Liu, J. J., Chi, Q. G., Zhai, J. W., et al. (2021). Ultrahigh energy storage performance of layered polymer nanocomposites over a broad temperature range. *Advanced Materials*, 33: 2103338.

[174] Chi, Q. G., Gao, Z. Y., Zhang, T. D., Zhang, C. H., Zhang, Y., Chen, Q. G., Wang, X., Lei, Q. Q. (2019). Excellent energy storage properties with high-temperature stability in sandwich-structured polyimide-based composite films. *ACS Sustainable Chemistry & Engineering*, 7: 748–757.

[175] Thakur, Y., Zhang, T., Iacob, C., Yang, T. N., Bernholc, J., Chen, L. Q., Runt, J., Zhang, Q. M. (2017). Enhancement of the dielectric response in polymer nanocomposites with low dielectric constant fillers. *Nanoscale*, 9: 10992–10997.

[176] Zhang, T., Chen, X., Zhang, Q. Y., Zhang, Q. M. (2020). Dielectric enhancement over a broad temperature by nanofiller at ultralow volume content in poly(ether methyl ether urea). *Applied Physics Letters*, 117: 072905.

[177] Zhang, T., Chen, X., Thakur, Y., Lu, B., Zhang, Q. Y., Runt, J., Zhang, Q. M. (2020). A highly scalable dielectric metamaterial with superior capacitor performance over a broad temperature. *Science Advances*, 6: eaax6622.

[178] Fan, M. Z., Hu, P. H., Dan, Z. K., Jiang, J. Y., Sun, B. Z., Shen, Y. (2020). Significantly increased energy density and discharge efficiency at high temperature in polyetherimide nanocomposites by a small amount of Al_2O_3 nanoparticles. *Journal of Materials Chemistry A*, 8: 24536–24542.

[179] Yuan, C., Zhou, Y., Zhu, Y., Liang, J., Wang, S., Peng, S., Li, Y., Cheng, S., Yang, M., Hu, J., et al. (2020). Polymer/molecular semiconductor all-organic composites for high-temperature dielectric energy storage. *Nature Communications*, 11: 3919.

[180] Luo, S. B., Yu, J. Y., Ansari, T. Q., Yu, S. H., Xu, P. P., Cao, L. Q., Huang, H. T., Sun, R., Wong, C. P. (2020). Elaborately fabricated polytetrafluoroethylene film exhibiting superior high-temperature energy storage performance. *Applied Materials Today*, 21: 100882.

[181] Luo, S. B., Ansari, T. Q., Yu, J. Y., Yu, S. H., Xu, P. P., Cao, L. Q., Huang, H. T., Sun, R. (2021). Enhancement of dielectric breakdown strength and energy storage of all-polymer films by surface flattening. *Chemical Engineering Journal*, 412: 128476.

[182] Zhang, X. M., Zhao, Y. F., Wu, Y. H., Zhang, Z. C. (2017). Poly(tetrafluoroethylene-hexafluoropropylene) films with high energy density and low loss for high-temperature pulse capacitors. *Polymer*, 114: 311–318.

[183] Chen, S. Y., Meng, G. D., Kong, B., Xiao, B., Wang, Z. D., Jing, Z. A., Gao, Y. S., Wu, G. L., Wang, H., Cheng, Y. H. (2020). Asymmetric alicyclic amine-polyether amine molecular chain structure for improved energy storage density of high-temperature cross-linked polymer capacitor. *Chemical Engineering Journal*, 387: 123662.

[184] Wen, F., Zhang, L., Wang, P., Li, L. L., Chen, J. G., Chen, C., Wu, W., Wang, G. F., Zhang, S. J. (2020). A high-temperature dielectric polymer poly(acrylonitrile butadiene styrene) with enhanced energy density and efficiency due to a cyano group. *Journal of Materials Chemistry A*, 8: 15122–15129.

[185] Zhou, Y., Yuan, C., Wang, S. J., Zhu, Y. J., Cheng, S., Yang, X., Yang, Y., Hu, J., He, J. L., Li, Q. (2020). Interface-modulated nanocomposites based on polypropylene for high-temperature energy storage. *Energy Storage Materials*, 28: 255–263.

[186] Wang, Y. G., Zhang, J. X., Zhang, B. W., Ren, K. L. (2021). Poly(lactic acid)-based film with excellent thermal stability for high energy density capacitor applications. *Macromolecular Materials and Engineering*, 306: 2100402.

[187] Yang, Y., Dang, Z. M., Li, Q., He, J. L. (2020). Self-healing of electrical damage in polymers. *Advanced Science*, 7: 2002131.

[188] Liu, Y., Yang, T. N., Zhang, B., Williams, T., Lin, Y. T., Li, L., Zhou, Y., Lu, W. C., Kim, S. H., Chen, L. Q., et al. (2020). Structural insight in the interfacial effect in ferroelectric polymer nanocomposites. *Advanced Materials*, 32: 2005431.

[189] Tan, D. Q. (2020). Review of polymer-based nanodielectric exploration and film scale-up for advanced capacitors. *Advanced Functional Materials*, 30: 1808567.

[190] Sharma, V., Wang, C., Lorenzini, R. G., Ma, R., Zhu, Q., Sinkovits, D. W., Pilania, G., Oganov, A. R., Kumar, S., Sotzing, G. A., et al. (2014). Rational design of all organic polymer dielectrics. *Nature Communications*, 5: 4845.

[191] Mannodi-Kanakkithodi, A., Treich, G. M., Huan, T. D., Ma, R., Tefferi, M., Cao, Y., Sotzing, G. A., Ramprasad, R. (2016). Rational co-design of polymer dielectrics for energy storage. *Advanced Materials*, 28: 6277–6291.

[192] Kern, J., Chen, L. H., Kim, C., Ramprasad, R. (2021). Design of polymers for energy storage capacitors using machine learning and evolutionary algorithms. *Journal of Materials Science*, 56: 19623–19635.